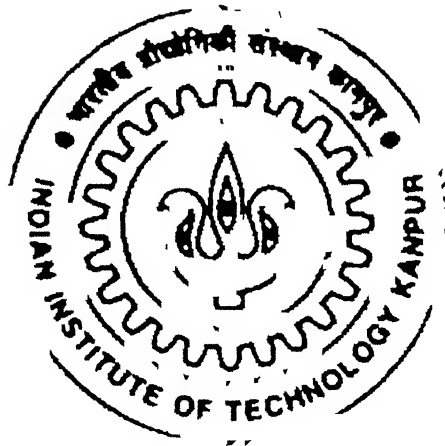# DEFORMATION TEXTURES AND MICROSTRUCTURES IN Ni-Co ALLOYS

by

SRIKANTA KUNDU

DEPARTMENT OF MATERIALS AND METALLURGICAL ENGINEERING

Indian Institute of Technology, Kanpur

DECEMBER, 1999

DEFORMATION TEXTURES AND MICROSTRUCTURES IN Ni-Co ALLOYS

A Thesis Submitted
in Partial Fulfilment of the Requirements
for the Degree of

MASTER OF TECHNOLOGY

by

SRIKANTA KUNDU
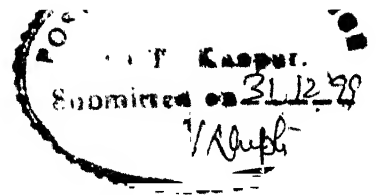
To the

DEPARTMENT OF MATERIALS AND METALLURGICAL ENGINEERING

Indian Institute of Technology, Kanpur

DECEMBER, 1999

CERTIFICATE

This is to certify that the present work, entitled **DEFORMATION TEXTURES AND MICROSTRUCTURES IN Ni-Co ALLOYS** by Mr. Srikanta Kundu has been carried out under our supervision and to the best of our knowledge it has not been submitted elsewhere for a degree.

Dr. R.K. Ray
Professor
Dept. of Materials & Metallurgical Engg.
Indian Institute of Technology
Kanpur

Date: 31/12/99

Dr. Deepak Gupta
Associate professor
Dept. of Materials & Metallurgical Engg.
Indian Institute of Technology
Kanpur

Date: 31/12/95

Acknowledgement

December 31,1999
I.I.T. Kanpur

Srikanta Kundu
(9810624)

Synopsis

Cold rolling textures developed in Ni-Co alloys with varying Co content show transition from pure Cu type to α brass type. The textures developed in pure Ni and Ni-Co alloys with upto 30%Co are pure metal type at all deformation levels from 40% to 95%. Ni-60%Co develops α brass type texture at all deformation levels. The intermediate texture developed in Ni–40%Co shifts from pure metal type to α brass type with increasing deformation. The texture transition observed in the Ni-Co system is found to be very much similar to that known for Cu-Zn system. The transition in texture from pure metal type in pure Ni to α brass type in Ni-60Co is believed to be due to the drastic reduction of stacking fault energy of pure Ni brought about by Co in solid solution.

Contents

List of Figures

List of Figures

List of Tables

Chapter 1

Introduction

Ni-base alloys constitute a group of soft magnetic materials of commercial importance. The most common amongst these is "Permalloy" which contains about 78 percent Ni. Magnetic property is anisotropic and in Ni the direction of easy magnetization is the <111> direction, the diagonal of the face centered cubic unit cell. The enhancement of magnetic properties is hence a strong function of the crystal orientation or "texture" developed in these materials during processing.

Preferred orientation or "texture" is strongly dependent upon the crystal structure as well as the processing parameters. In closed packed structures, as in the case of fcc unit cell of Ni, the stacking fault energy also influences the development of texture. In fcc metals and alloys three types of deformation textures are usually identified:

(i) brass or alloy type texture in low stacking fault energy materials

(ii) copper or pure metal type texture in medium stacking fault energy materials and

(iii) aluminium type texture in very high stacking fault energy materials.

The brass-type has practically only the brass component {011}<211>. In the copper type the Cu {112}<111>, Bs {011}<211> and S {123}<634> components are nearly equally strong, whereas in the case of aluminium type the S {123}<634> component predominates.

The stacking fault energy of Ni has been reported to be 130 mJ/m^2 [1] as compared to 200 mJ/m^2 for Al. Deformation texture of pure Ni is similar to that of Cu. The addition of Co to Ni in solid solution reduces the stacking fault energy of Ni drastically [4]. The influence of this change in SFE to the development of texture in Ni-Co system is yet to be extensively investigated. The previous work on this system was

1.   *Introduction*

carried out for 95% cold rolled pure Ni , Ni-10%Co, Ni-20%Co, Ni-30%Co, Ni-40%Co and Ni-60%Co alloys [2]. The investigation revealed that for 95% cold deformation the texture developed in the set of Ni-Co alloys with upto 30%Co addition were similar to that developed in pure Ni i. e. Cu or pure metal type texture while the 60%Co alloy shows alloy type texture. The rolling texture of Ni-40%Co alloy lies in between these two extremes. The texture transition in the Ni-Co alloys has been attributed to the additional effect of the incidence of twinning caused by the sharp decrease of stacking fault energy of Ni by Co-addition. The present work has been taken up with the same set of alloys cold rolled to four different levels of deformations 40%, 70%, 90% and 95%. The objective was to investigate the effect of Co in solid solution to the texture developed at low, medium & high levels of cold rolling in these alloys. The course of development of texture from low to high deformations in any of the Ni-Co alloys under investigation could also be studied under the present work plan. Similar work on deformation textures has been carried out for Cu base Cu-Zn alloys [3] but no such investigation has yet been reported for Ni base Ni-Co alloys. Thus the present work is expected to reveal a lot about the whole phenomenon of deformation texture development in Ni-base Ni-Co alloys.

Chapter 2

Literature Review

2.1 Ni-Co System

In the periodic classification of elements, cobalt and nickel both occur in the first long period (period 3) of the transition group VIII.

Table 2.1   Physical Properties of Nickel and Cobalt.

Properties	Nickel	Cobalt
Symbol	Ni	Co
Atomic Number	28	27
Atomic Weight	58.71	58.93
Crystal	FCC	FCC
Density	8.9 gm/ml	8.9 gm/ml
Melting Point	1453°C	1495°C
Boiling Point	2730°C	2900°C
Electron Structure	[Ar] $3d^8$ $4s^2$	[Ar] $3d^7$ $4s^2$
Lattice Parameter	3.5238 Å	3.552 Å

Nickel forms a continuous series of solid solutions with Co at temperatures upto 1495°C. Fig [2.1] shows the phase diagram of the Ni-Co system. The Curie temperature is 361°C in pure Ni and that for pure Co is 1121 °C. Co increases the curie temperature in Ni almost linearly with wt%. It also increases the resistivity of Ni.
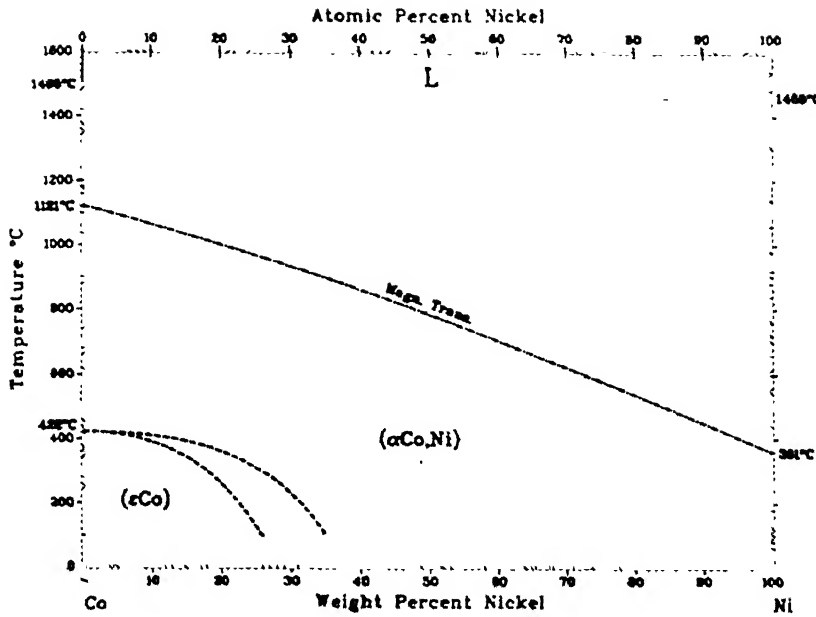
Figure 2.1   Phase diagram of the Ni-Co system

Soft magnetic materials are those which are readily magnetized to saturation in a weak magnetic field and which also lose their magnetism readily on removal of the field. Ni is extensively used in soft magnets because of its exceptional high permeability value. The maximum is reached for 78% Ni which forms the basis of a group of alloys termed "Permalloy". Special versions of these alloys are produced by developing grain oriented structures during cold working and heat treatment. Figure 2.2 shows the magnetization curves of Ni in different crystallographic directions. The easy direction of magnetization in Ni is the <111> or the body diagonal of the face centred unit cell. Grain orientation essentially involves producing textured material with grains alligned in the direction of easy magnetization to produce magnets with better permeability.
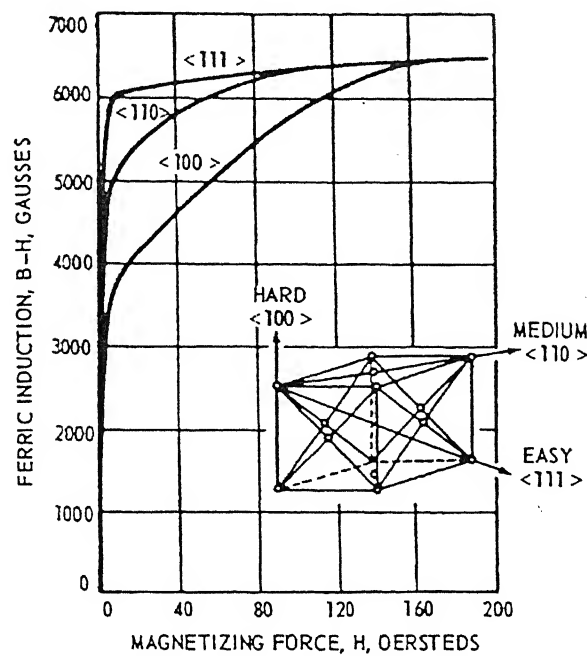
Figure 2.2   Magnetization curve of Ni in different crystallographic directions[5]

2.2 The Cold Worked State

Generally the cold-worked state may be taken as any strained or damaged condition of a crystalline material brought about by processes such as plastic deformation, particle bombardment, quenching from a high temperature or phase transformations[6] . The entities responsible for the cold worked state are point defects such as vacancies and interstitials as well as linear and planar defects like dislocations and stacking faults, etc. In the present review only the cold worked state produce by plastic deformation will be discussed in general, with reference to fcc metals and alloys. Plastic deformation of a material involves a permanent shape change produced by stressing the material beyond its elastic limit. Any or all of the types of defects mentioned above may be produced in the solid during the course of plastic deformation. If the deformation occurs at sufficiently low temperature , many of these defects will be retained and the material is now in a thermodynamically metastable state.

2.3   Preferred Orientation or Texture

Metals of industrial practice are polycrystalline aggregates in which each of the individual grains has an orientation that differs from those of its neighbours. It is quiet unusual for the grains in such metals to have a random distribution of orientations, and the non-random distributions that occur are called "Preferred Orientation" or Textures [7]. Textures develop at all stages of manufacturing process of metals. Textures created during deformation depend on the crystal structure as well as the nature and severity of the working process. Moreover, in the case of closed packed structures such as fcc metals the stacking fault energy also influences the texture. When a polycrystalline material is plastically deformed the lattice orientation in individual grains is found to rotate and the material thereby assumes a preferred orientation. The nature of the preferred orientation or the texture which the material acquires is characteristic of the material itself and also depends on the variable connected with the deformation process. The most complete description of texture of a polycrystalline material is given by stating the crystallographic orientation of each and every crystallite belonging to it. This is virtually impossible so it is customary to use a statistical description. X-ray diffraction methods are widely used to yield a collective determination of orientations over a large number of crystals through scan and integrating mechanisms. The data is normally represented by the use of conventional or inverse pole figures or by means of mathematical functions. The information given by a conventional pole figure is conveniently expressed in terms of "ideal orientations" of the form {hkl}<uvw> where {hkl} denotes the indices of the crystallographic plane in the plane of the sheet and <uvw> the direction parallel to the rolling direction.

Mathematical techniques for the representation of preferred orientation have also been proposed principally by Bunge [8]and Roe[9]. The mathematical process involves the formation of a distribution function of orientation from a set of suitably processed data of several individual pole figures. A complete description of texture is provided by a function that describes the orientation of all the crystallites in the metal which is called the Orientation Distribution Function (ODF).

2.4   Rolling Texture of FCC Metals and Alloys

The rolling texture of fcc metals, fall into two principal types. The "pure metal or Cu" texture occurs in most pure metals e.g. Cu, Ni, Al & Au. The "alloy or brass" texture is found in many alloys of these metals and also in pure Ag [7]. Fig 2.3 shows the (111) pole figures for Cu and 70:30 brass cold rolled under similar conditions revealing Cu type and brass type texture developed in the respective cases.
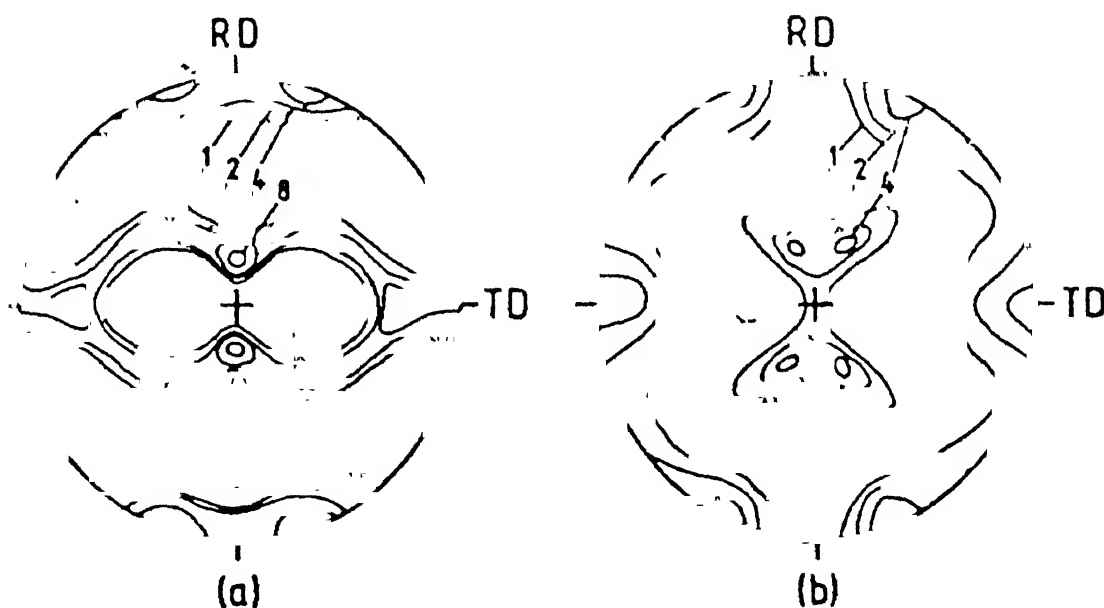
Figure 2.3   (111) pole figure of pure Cu (a) and 70:30 brass (b).

Beck and his co-workers [10,11] made quantitative texture determination on Cu, Al and α-brass after 96% cold reduction. They found that the rolling texture of Cu and Al are similar but are different from that of α-brass (Fig 2.3 (b)). The α-brass texture could be characterized by the ideal orientation {110} <112> plus a minor {110} <001> component. The Cu and Al texture could not be described readily and the texture for Cu has been called an irrational texture. Hu, Sperry and Beck [11] suggested an 'ideal orientation' of approximately {123} <412> to designate the type of texture encountered in Cu and Al using quantitative pole figures. To account for the intensity maxima in the pole figures, a second ideal orientation of near {146} <211> was also used to describe the texture of Cu. The results of a number of texture studies [12-19] indicate that the texture

of most fcc metals (except Ag) are of the Cu type whereas those of the Ag and most fcc alloys are of the brass-type.

In an elastically anisotropic material, such as Cu for which single crystal moduli are available, measurements of Young's modulus was used to interpret texture data. Weerts [20] assumed the texture of Cu to consist of equal volumes of {110} <112> and {112}<111>, and calculated the variation of Young's modulus with direction. He obtained reasonable agreement with the measured variation. Jones and Fell [21] deduced that the theoretical modulus variation with direction for the ideal orientation {123} <412> did not fit the experimental data. They too preferred to describe the rolling texture of Cu as a mixture of {110} <112> and {112} <111>. Lucke, Perlwitz and Pitsch [22] and Haessner, Jakubowski and Wilkens [23] independently made useful contributions to the study of texture in polycrystalline fcc metals. These workers made orientation determination by selected area diffraction techniques of the crystallites in a polycrystalline Cu- sheet rolled to 95% reduction. A statistical analysis of the orientation distribution measurements made on several hundred spots over a large area of the sample were made. The distribution of poles as deduced from the SAD data was found to be in essential agreement with the X-ray pole figures.

2.5   Texture Transition in FCC Metals and Alloys

Smallman [12-19], Liu and Richman [17,18] and others have extensively investigated the effect of solute additions on the deformation textures of a number of fcc metals. That the texture transition from Cu to α-brass type was caused by the addition of elements like Al, Zn and Ge was shown by Smallman. Liu and Richman confirmed the transition by addition of the elements P, As, Sb,Ge and Sn to copper. Clark et. al. [24] have shown that pure Ni has a texture similar to that of Cu. However gradual transition have been found to an α-brass type of texture where Co is added to Ni in solid solution [13,14].

That a minimum amount of solute is required to initiate texture transition, was shown by Smallman and Liu. They showed that for a given solute the degree of transition increases with increase in solute concentration. For complete transition a minimum amount of solute is required which varies from solute to solute. Any further addition of solute does not change the texture. Smallman [12] tried to correlate the amount of solute

solvent elements. He found that for a given solvent metal, the greater the misfit of the solute atoms in the solvent lattice, the lower the concentration required to complete the texture transition. This finding made Smallman deduce that elastic interaction between the solvent and the solute atoms is the most important factor in affecting the mode of deformation and hence the texture. Liu and Richman [17,18] on the other hand suggested that the combination of electronic and ion-core interaction might be more important than elastic interaction in initiating a texture transition. Fig 2.4 shows a typical texture transition of Cu to α-brass type, on the additions of increasing amounts of Zn to Cu.

(a) 3% Zn   (b) 6% Zn   (c) 10% Zn
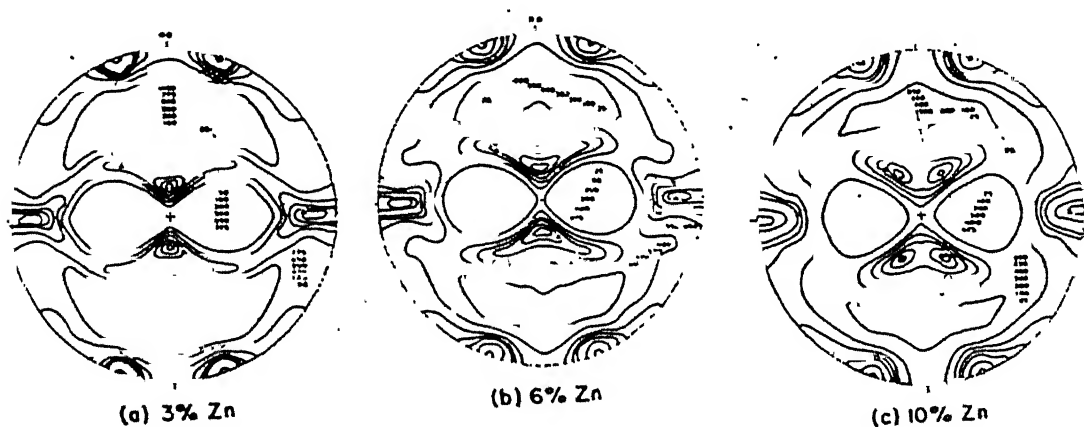
Figure 2.4   (111) pole figures showing texture transition in cold rolled Cu on the addition of different amount of Zn

For characterization of fcc preferred orientation over the range from the Cu type or pure metal type to the α-brass or alloy type, a number of parameters have been devised. Smallman's [12] suggestion was based on a ratio of intensities near the centre of the (111) pole figure. A second parameter suggested by Liu and Richman [18] was based on the ratio of intensities on the periphery of the (111) pole figure at the transverse direction I_{TD} to that 20° from the rolling direction I_{20}. This parameter was supposed to be more sensitive than Smallman's and was used by Dillamore et. al. [25]. Texture of various fcc pure metals rolled 95% at room temperature are listed in Table 2.2 with a qualitative as well as quantitative description in terms of the parameter (I_{TD}/I_{20}). The amount of various

solute elements required for complete texture transition from 'pure metal' type to 'alloy' type in all these metals are also indicated in this table.

Table 2.2 Effect of alloying on deformation texture of various metals[26].

Metal	Texture	I_{TD}/I_{20}	At% solute to transform to alloy texture for 95% deformation.
Al	Pure-metal	0.42	-
Cu	Pure-metal	0.72	20%Zn, 8%Al, 4%Ge, 3.5%Sn, 2%P
Au	Pure-metal	0.75	8%Zn
Pb-2%Ca	Pure-metal		-
Ni	Pure-metal	0.49	50%Co, 10%Mo
Pd	Pure-metal	0.55	-
Pt	Intermediate	0.94	-
Rh	Pure-metal	0.67	-
Ag	Alloy	1.31	-
Th	Pure-metal	0.7	90%Ce
Yb	Alloy	1.30	-

There is also evidence that raising the temperature of deformation above room temperature can also affect texture transition. Pure Ag has been found to develop a texture similar to that of α-brass when rolled at room temperature, whereas when rolled at elevated temperatures it assumes a texture similar to that of pure Cu.

As determined from X-ray peak-shift measurements, Hu and co-workers [27-29] suggested a general correlation between the temperature dependence of rolling texture transition and stacking fault frequency or probability. According to them the brass-type textures are associated with high stacking fault frequencies, whereas the copper type textures are associated with relatively low stacking-fault frequencies. The transition of Cu-type to the brass type texture that occurs on alloying was related to a decrease in stacking fault energy by Smallman and Green [30] using Cu-Al and Cu-Ge alloys. Haessner [14] employed a similar correlation for the texture transition that takes place when Co is added to Ni.

Texture development in cold rolled Cu and α–brass has been extensively investigated as a function of rolling reduction by Hirsch and Lücke [3]. They based their analysis on ghost corrected three dimensional ODFs with the help of Gauss model calculations. They observed that there is no unique and simple method of describing rolling texture development which is applicable to the whole range of deformations. At

low degrees of rolling the textures of all investigated alloys are very similar and can be best described by orientation concentrations along two fibres, the α fibre (<110> direction parallel to the sheet normal) and the β fibre (<110> direction tilted 60° towards rolling direction). With increasing degree of rolling, this fibre structure deteriorates and along the fibres which were originally homogeneously occupied, pronounced maxima form. These structures are characterized by strong peaks and can be described rather well by components with Gauss type scattering.

Similar work has been done by Ray[2] with 95% cold rolled Ni base Ni-Fe and Ni-Co alloys with varying Fe and Co alloys. His analysis of ghost corrected ODFs with the help of Gauss model calculations showed the similarity in texture developed in all Ni-Fe alloys under study. In case of the Ni-Co alloys Cu type texture was observed in alloys upto 30% Co whereas the texture in Ni-60%Co resembled that of α brass. The texture in Ni-40%Co was found to be mid-way between the Cu and the α brass type, thus showing a texture transition with Co addition. Ray concluded that the addition of Co to Ni reduces the stacking fault energy to such an extent that at 40% Co addition a transition in texture initiates which transforms the Cu type texture of pure Ni to the brass type texture in Ni-60%Co. Such transition in rolling texture is not observed in case of the NI-Fe alloys since Fe brings about only a small change in the stacking fault energy in Ni.

2.6 Theories of Texture Development in FCC Metals and Alloys

Theories of texture development have been proposed by Wever and Schmid, Boas and Schmid, Pickns and Mathewson, Taylor, Hibbard and Yen. These earlier theories have been adequately reviewed by Barret [20] and Underwood [31]. The later theories have been reviewed in detail by Dillamore and Roberts [26], Hu, Cline and Goodman [32] and Haessner [33]. The four more resent theories of texture formation in fcc metals and alloys more or less make use of the concept of stacking fault energy in the development of texture. All these theories used the basic principles or method of analysis used in earlier theories of deformation texture. Haessner [34] proposed that texture transition in fcc metals and alloys is caused by non-octahedral slip. According to him, normal octahedral

slip will lead to the {110}<112> or brass type texture. Copper type texture will be developed if slip can also occur on the {100} planes in the <110> direction as an additional deformation mode to {111} slip. Haessner's proposition is similar to the mechanism suggested earlier by Richard's and Pugh [35] to explain the ideal orientation {112} <111>. They assumed that second shear in the {100}<110> system following normal octahedral slip would change the {110}<112> orientation into {112}<111>. It was further proposed by Haessner that for metals with low stacking fault energy, cubic slip will become more difficult as the separation of the particles in the {111} planes become wider.

A theory based on dislocation interaction has been proposed by Liu [36] to explain the formation of rolling textures in fcc metals and alloys. He considered that during deformation the slip systems which operate are determined by the ability of dislocations on these slip systems to interact, producing a net reduction of energy. Having determined which sets of four slip systems give the greatest reduction in energy, the end texture is the orientation at which the slip rotations on the operating systems cancel out. On this basis, Liu predicted that for metals of low stacking fault energy, the ideal orientations were {110}<112> plus an orientation spread with (110) in the rolling plane. The ideal end orientation for metals of high stacking fault energy was shown to be close to {358}<523>.

Hu et. al. [32] pointed out that although these results were in essential agreement with the two types of rolling textures observed in fcc metals or alloys, the {112}<111> orientation of the copper type texture was not predicted from Liu's analysis. This theory has also been criticized on the grounds that there would, in fact, be no net reduction in internal energy due to interactions of dislocations on the operating systems. The main difficulty with Liu's theory is that it is highly hypothetical and the present scientific knowledge and experimental techniques available are not sufficient to test the validity of the postulates of his theory. Dillamore and Roberts [37] proposed their cross slip hypothesis in order to explain the deformation textures in fcc metals and alloys. They suggested that all fcc metals first develop the {110}<112> or the brass type texture by normal slip. The Cu type pure metal texture is formed if, in addition to {111} slip on the primary and on the secondary systems, large amounts of cross slip also takes place on other planes.

A strong objection to the cross slip hypothesis was put forward by Haessner. He pointed out [33] that the internal stress attained in rolling is largely dependent on the stacking fault energy of the materials and is much higher than $\tau_{111}(0)$, the stress at which cross slip starts to occur in single crystals at $0^{\circ}K$. He based his arguments on the cross slip models of Schöck, Seeger and Wolf[38,39] and also on that of Hirsch(40). Geometrically, equal proportions of slip on two {111} planes, e.g. the primary and the cross slip plane is equivalent to cubic slip. Thus the theories of Haessner and Dillamore and Roberts lead to essentially the same model that is capable of explaining the textures of fcc metals and alloys geometrical.

The 'twin hypothesis' of Wassermann [41] is quite different from the slip theories already mentioned. In this theory mechanical twining is supposed to be responsible for the observed texture transition in fcc metals and alloys. He assumed that during deformation, all metals tend to develop the copper type or pure metal texture by means of slip on {111} planes. For the development of brass type texture, mechanical twinning, as an additional deformation mode is essential. He proposed that the rolling texture of fcc metals can be considered as being composed of two limited fibre textures centred on the orientation {110}<112> and {112}<211>. If mechanical twining in the systems {111}<211> is considered as a possible deformation mode additional to normal slip, then the material in the {112}<111> orientation may be transformed by twinning to the {552}<115> orientation, which rotates into the {110} <001> orientation by subsequent slip. Wassermann argued that {110}<112> orientation does not change during deformation, because twinning of this orientation would lead to shape change that do not meet the strain requirements of the rolling process. The proposed mechanism is in agreement with the observation that metals of low stacking fault energy may deform by mechanical twinning [42] and it is these metals which exhibit the 'alloy texture'. The theory is also consistent with the observations on the temperature dependence of twinning of fcc single crystals.

Chapter 3

Experimental Procedure

3.1 Material and Initial Treatment

The chemical composition of the alloys (wt%) used in the present study are given in the following table. Both the nominal as well as the detailed compositions of the alloys are shown.

Alloy	Nominal composition	Detailed composition (wt%)						
		Fe	Co	C	S	Si	Cu	Ni
A	Ni	0.18	-	0.007	0.003	0.06	0.04	Balance
B	Ni-10%Co	-	11.15	0.006	0.003	0.03	0.03	Balance
C	Ni-20%Co	-	22.85	0.007	0.003	0.06	0.03	Balance
D	Ni-30%Co	-	30.90	0.006	0.003	0.03	0.03	Balance
E	Ni-40%Co	-	41.05	0.006	0.004	0.03	0.03	Balance
F	Ni-60%Co	-	60.50	0.006	0.004	0.06	0.03	Balance

Table 3.1   Chemical compositions of alloys (wt%)

All the alloys were melted under vacuum in an induction furnace using virgin metals of 99.99% purity. Magnetic stirring was resorted to during melting to avoid segregation. Cylindrical ingots of 20mm height were cast under argon atmosphere. The ingots were cold rolled 50% to a thickness of 10mm and then homogenization annealing was performed in vacuum at 1150°C for 24 hrs. Further cold rolling to 50% was performed followed by annealing at 1100°C (for alloys B-F) and at 800°C for alloy A for a period of 3hrs. to yield the starting material of almost random texture and a grain size of 0.1 mm.

3.2   Cold Rolling

Strips cut from the starting materials for all the alloys were cold rolled using a laboratory rolling mill having 250mm diameter rolls. The ratio of the length of contact with the rolls to specimen thickness was maintained at a value greater than unity in order to get homogeneous deformation throughout the specimens. During rolling the strips were reversed end to end after each pass and between two successive passes the strips were immersed in cold water to reduce the temperature rise due to deformation. Each alloy was rolled to four different deformation levels of 40%, 70%, 90% and 95% final reduction in thickness.

3.3   Optical Microscopy

The cold rolled samples were cold mounted for examination under the optical microscope. The samples for optical microscopy were ground and polished on emery papers (0 to 4 grades) followed by wet polish with alumina suspension of particle size $1\mu m$ and $0.05\mu m$ respectively. These were subsequently etched before examining the microstructure. The etching reagents used are :

(a)   glacial acetic acid and concentrated HNO_3 mixed in the ratio 1:1,

(b)   two gm anhydrous $FeCl_3$ in 96 ml ethanol and 2 ml HCl.

Microstructures were recorded from the rolling, transverse and longitudinal sections of the samples. All the microstructures were photographed with the help of Leitz Metallux microscope having camera attachment.

3.4   Determination and Representation of Texture

The crystallographic texture in a rolled polycrystalline material is usually represented as {hkl}<uvw>, where {hkl} represents the set of planes of the crystal that are parallel to the rolling plane and <uvw> represents the set of directions that are along the rolling direction. Texture in a specimen may consist of a number of components and it is generally reported in the form of pole figures. A better way of representing texture is through the use of Orientation Distribution Function (ODF) which provides a more

quantitative description of texture than a pole figure. An ODF describes the frequency of occurrence of orientations in three dimensional orientation space (Euler space) which is defined by the three Euler angles ϕ_1, ϕ and ϕ_2. These angles are three consecutive rotations which transforms the specimen frame S, to the crystallographic frame C as shown in Fig 3.1.
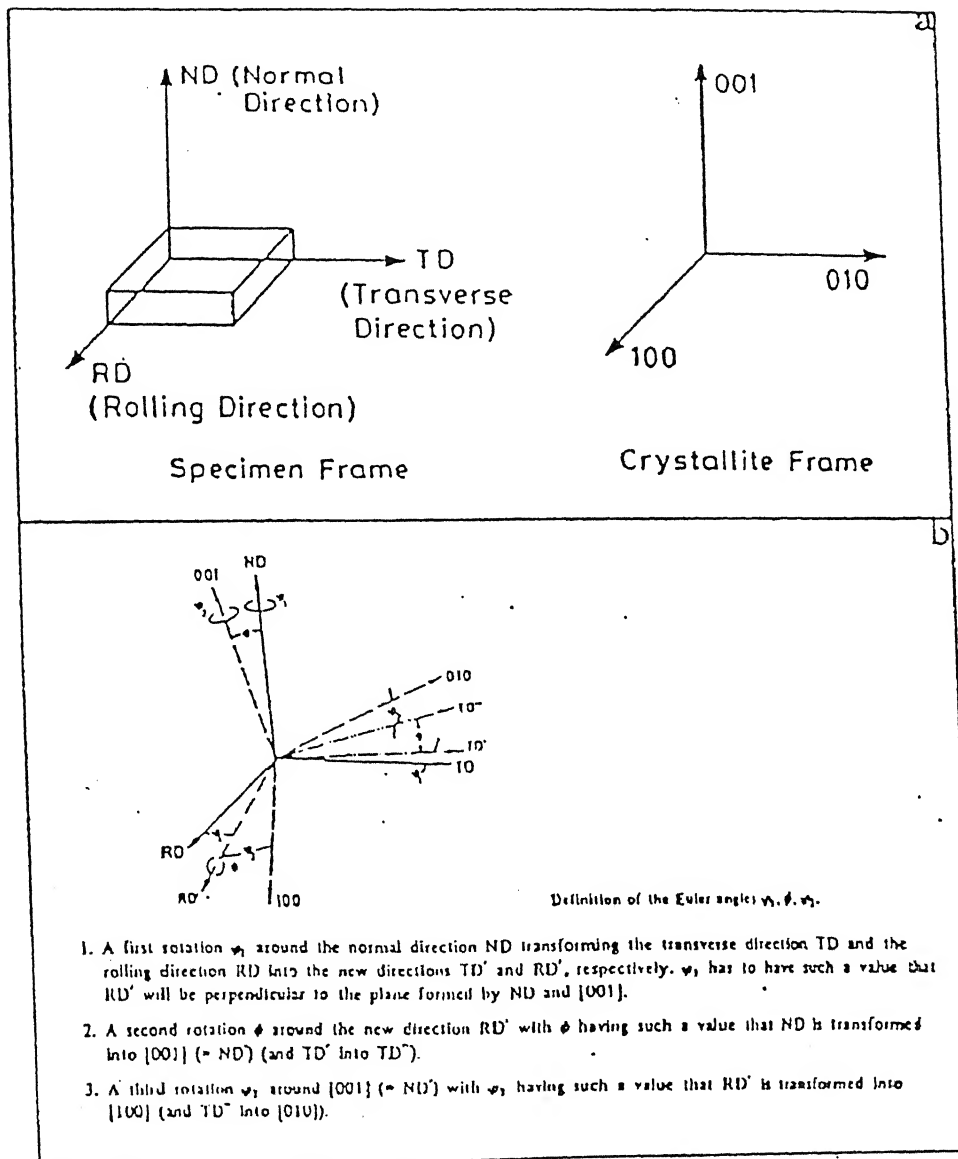

Fig 3.1   Schematic representation of three Euler angles ϕ_1, ϕ, ϕ_2 ; (a) specimen frame S and crystallite frame C, (b) transformation of specimen frame into crystallite frame.

Any particular texture component {hkl}<uvw> can be completely represented by a point
(ϕ_1, ϕ, ϕ_2) in the Euler space. Each texture component has a distinct position in the
orientation space and as a result the quantitative analysis of texture with a much better
resolution is possible using the ODF method. The schematic diagram of the Euler space
is shown in Fig 3.2.
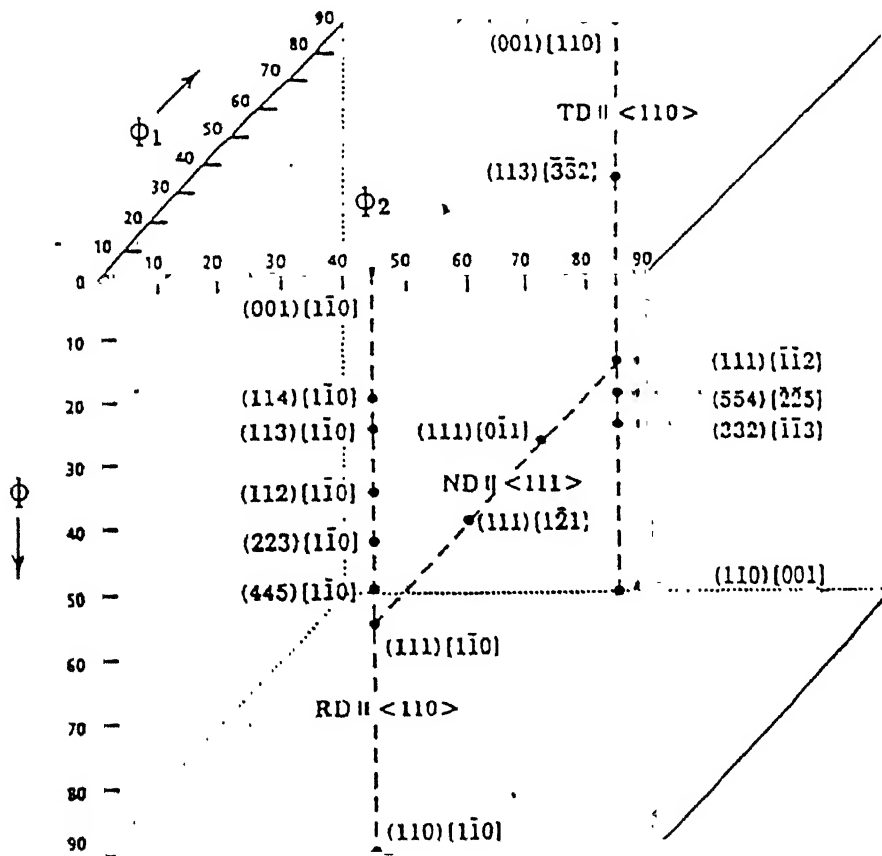
Fig 3.2   Schematic presentation of Euler Space.

The experimental pole figure data are converted to ODF through mathematical methods
developed by Bunge[8] and Roe[9] who used spherical harmonic functions to represent
orientation distribution. In the Bunge notation which is more commonly used in
texturestudy the orientation space is defined by three orthogonal axes ϕ_1,ϕ,ϕ_2 each

ranging from 0° to 90°. This total volume is divided into three basic ranges in which each orientation appears only once. The value of the orientation density at each point is the intensity of that orientation in multiples of the random.

Reproducible texture was found over almost the whole thickness of the samples under study except in a very narrow zone near the outermost surface. From each specimen, material was etched off from one side up to the mid-thickness, on which texture measurements were carried out. Texture measurements were performed on $14X24$ mm^2 rectangular specimen of the various samples under study. The texture was determined by plotting ordinary pole figures as well as orientation distribution function (ODF). From each texture sample pole figures were measured using Cu K_α radiation, in the range of azimuth angles 5° to 85°. ODF was calculated from four incomplete pole figures $\{111\}$, $\{200\}$, $\{220\}$ and $\{311\}$ measured from each texture sample.

Chapter 4

Experimental Results

4.1 Study of Optical Micrographs

Figures 4.1 – 4.6 show optical micrographs taken from the longitudinal sections of the samples under study. In all the alloys the microstructures for 40% and 70% cold rolling show distinct grains with delineated grain boundaries. Twin like features are visible in pure Ni as well as all the Ni-Co alloys right from the lowest level of deformation. The sections show elongated grains as expected from the longitudinal sections of rolled material. Deformation bands are clearly visible in the 70% deformed structures but are not so common at 40% deformation.

At 90% deformation, grains can no longer be distinguished in any of the samples. The structure at 90% and 95% deformation in all alloys show profusion of deformation bands as is typical of heavily deformed structures. The deformation bands are thinner and more fragmented in the 95% deformed structures.

4.2 Study of Crystallographic Texture

The cold rolling texture of the samples under study was characterized with the help of pole figures and ODFs. All measurements were carried out on the mid-thickness section in 14x24 mm^2 rectangular specimens by etching material off from one side. The equipment used for texture measurement was a SIEMENS texture goniometer using Cu K$_\alpha$ (λ=1.542Å). Four incomplete pole figures – {111}, {200}, {220}& {311} were measured from each samples and from these, three dimensional ODFs were calculated after correction and symmetrization using the series expansion method[9,43,44] with a

limit of l_{max}=22. The resulting ODFs were approximated by model ODFs consisting of a superposition of isotropically scattering Gauss distributions [45-48]. This procedure made it possible to describe the rather complicated looking texture plots by only a few parameters, such as the volume fraction and peak density , f(g), of the Gauss type texture component. Model ODFs also help to correct the experimental ODFs of the so called "ghost error" especially in orientation regions of low intensity [49]. By the use of Gauss model the multiplicity of the different orientations is also automatically taken care of [3]. All ODFs analyzed have been corrected by the Gauss model method. A random background component has been included to take care of the additional weak components and irregular scattering.

4.2.1 Pole Figures

Figures 4.7 – 4.12 show the {111} pole figures for the rolling textures developed in pure Ni and the five Ni-Co alloys at the four deformations under study. In the Ni-Co alloys the {111} pole figures show similar nature as that shown by pure Ni upto 30% Co (Fig. 4.7 – 4.10). In any of these alloys a distinct course of development of texture is observed in the pole figures from 40% deformation to 95% deformation. At 95% deformation the pole figures of these three alloys match with those for rolled Cu (Fig2.3(a)) On the other hand the {111} pole figures of Ni-60%Co (Fig. 4.12) is completely different, and at 95% deformation it matches similarly with the {111} pole figure of cold rolled α brass (Fig2.3(b)). From 40% deformation to 95% deformation the {111} pole figures in Ni-60Co show the course of development of "alloy type" or 'brass'- type texture in these alloy. The {111} pole figures of Ni-40%Co (Fig. 4.11) show features common to both Cu-type and brass-type texture. It thus represents a transition texture from Cu-type to brass-type.

4.2.2 ODFs (Orientation Distribution Functions)

The composite ODF texture plots (Fig. 4.13-4.16) show that the texture in the relevant sections in Ni-Co alloys upto 30%Co are similar to that developed in pure Ni, but completely different to that in Ni-60Co. In these alloys as in pure Ni the Bs, Cu and S peaks do increase in intensity with deformation. From the ODF plots of Ni-40Co a

distinct change in texture is observed. The $\phi_2 = 0°$ section remains unchanged but the texture in the $\phi_2 = 45°$, $60°$ and $65°$ sections is quite different; particularly Cu peak in the $\phi_2 = 45°$ section shows drastic fall at higher deformations (Fig. 4.15-4.16) as compared to that in the alloys with lower Co content. The S intensity in the $\phi_2 = 60°$ and $65°$ section is also reduced. In the ODF plots of Ni-60Co the changes are more evident, for example, the Cu peak disappears in $\phi_2 = 45°$ section and the S spread is at its weakest. The Bs peak in the $\phi_2 = 0°$ section of Ni-60Co is very strong as compared to the other alloys. Thus the ODF section plots also reveal the contrasting texture developed in Ni-60Co as compared to the other Ni-Co alloys and Ni-40Co is again observed to show a transition texture state between the Ni-Co alloys upto 30Co on one hand and Ni-60Co on the other.

4.2.3 Texture Fibres

The comparison of rolling textures in different alloys is done through a detailed analysis of ODF results. In the ODFs of fcc metals and alloys, three fibre textures have been generally recognized which are actually a series of orientations lying on a tube running through the three-dimensional orientation space. Changes in the fibre textures can be quantitatively assessed by representing the orientation tube by its central line, called the skeleton line, and plotting intensity variations along these lines as a function of the orientation angle. The three fibres recognized in the alloys under study are:

- The α fibre, which starts at the goss (G) orientation $\{011\}<100>$ and passing through the Bs orientation $\{011\}<211>$, extends upto the $\{011\}<011>$ orientation. It is represented by its skeleton line extending from $\phi_1=0°$ to $\phi_1=90°$ for $\phi=45°$ in the $\phi_2=0°$ or $90°$ section of the ODF.

- The τ fibre stretches from $\{001\}<110>$ orientation and passing through the Cu position $\{112\}<111>$ goes up to the G orientation $\{011\}<100>$. Its skeleton line extends along the line $\phi=0°$ to $\phi=90°$ for $\phi_1=90°$ in the $\phi_2=45°$ section of the ODF.

- The β fibre runs from the Cu position $\{112\}<111>$, through the S orientation $\{123\}<634>$ and meets the α fibre at the Bs position. Here a skeleton line is

determined by connecting the density maxima in the different $\phi_2 =$ constant sections as a function of ϕ_2 [50].

Fig 4.17 shows the position of the three fibres mentioned above in the three-dimensional Euler space.
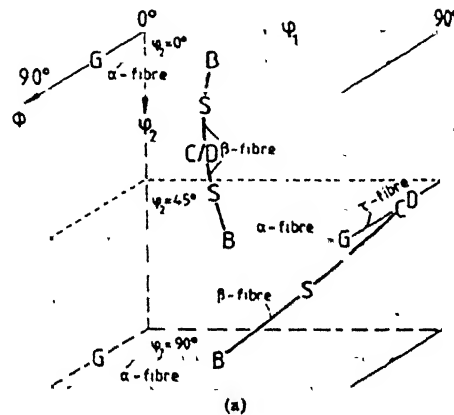
Figure 4.17   Position of the α, β and τ texture fibres in the Euler space.

α Fibre

The α fibre in case of Ni-Co alloys is inhomogeneous even at 40% deformation in contrast to pure Ni where it is homogeneous more or less upto 70% deformation (Fig. 4.18). The densities along the tube are affected both by degree of rolling and Co content. The G orientation shows minor variations with deformation. Upto 30Co it has tendency to decrease for higher deformations, at 40Co the density first decreases upto 70% and then increases with further cold rolling. But for 60Co a completely different trend is obtained where with increasing deformation the density increases continuously. The major increase is observed in the density of Bs {011}<211> component with deformation in all alloys of Co, except for 60Co in which case density falls beyond 90% deformation, same as in case of pure Ni. For any particular deformation the densities along the α fibre at Bs position reaches highest value for Ni-60Co (Fig. 4.19).

τ Fibre

The transformation of Cu type texture to Bs type texture is known to be caused by mechanical twins by which Cu orientations are transformed to a position near the G orientation. This leads to further increase in the G {011}<100> orientation which is visible in the τ fibre. For all alloys upto 30Co, deformation increase the density at the Cu orientation {112}<111> (Fig. 4.20). For 40Co the Cu intensity shows a decrease beyond 70% deformation accompanied by an increase at the G orientation. At 60Co intensity of the Cu orientation is non-existant where as there is a considerable rise at the G orientation. For Ni-60Co and 40Co (only 90 and 95% deformation) alloys an additional peak is observed near $\phi = 65°$, the appearance of which coincide with the decrease in the Cu intensity. Twin Cu at $\phi = 75°$ goes down with the decrease in Cu and a corresponding increase in G. Twin Cu is high in Ni-40Co 90% whence the Cu has just started to decrease in comparison to the other alloys. As twin Cu decrease a new maxima $\phi = 65°$ for all Ni-60Co alloys and 40Co 90 and 95% deformed, is observed.

β Fibre

The β tube shows a continuous increase in the density throughout its length at both Cu {112}<111> and Bs {011}<211> with deformation for 10, 20 and 30 Co (Fig. 4.22). A start in transition in the nature of the β tube is observed for Ni-40Co whence the Cu orientation shows a decrease in intensity beyond 70% deformation, accompanied by a growth in the Bs orientation. In 60Co the β tube has completely transformed and show a very low Cu orientation with respect to Bs orientation which is much pronounced compared to that in the other alloys. Thus where as the transformation in the β tube starts beyond 70% deformation in Ni-40Co it is already transformed at 40% deformation in Ni-60Co and much more pronounced (Fig. 4.23).

Course of the β Fibre

Fig. 4.17 shows the position of the β fibre in orientation space. The ϕ_1 and ϕ values of the density maxima in the various ϕ_2 sections are plotted which correspond to the position of

the β fibre skeleton line. The course of the β fibre in the various Ni-Co alloys under investigation is found to be not much different (Fig. 4.22). Deformation does shift the position of the density maxima in the various ϕ_2 sections of the orientation space but the shift is confined in each section within a narrow band of about $10°$ on both ϕ_1 and ϕ axes. Noteworthy is the behaviour observed in Fig. 4.23. At 40% deformation there is considerable scatter in the position of the β skeleton line in the various alloys. But with increased deformation the positions tend to converge and at 95% deformation the position of the β fibre coincides in all alloys matching with that in pure Ni. Thus at 95% deformation the major peaks for Cu, Bs and S in pure Ni and four Ni-Co alloys occupy exactly same positions.

4.2.4 Texture Components

A total of nine major and minor texture components have been identified in pure Ni and the five Ni-Co alloys under study from the analysis of ODF data. The standard nomenclature for the nine components and their {hkl}<uvw>, $\phi_1 \; \phi \; \phi_2$ values as used by Ray [2], Hirsch and Lücke[3] and Virnich[51] are given in table 4.1.

Table 4.1   Details of components identified in Ni-Co alloys

Name of Component	Symbol	{hkl}<uvw>	$\phi_1 \; \phi \; \phi_2$
Copper	Cu	{112}<1̄11>	(90,35,45)
Copper Twin - I	Twin Cu - I	{255}<5̄11>	(11,46,74)
Goss	G	{011}<100>	(0,45,0)
S	S	{123}<6̄34>	(59,37,63)
Brass	Bs	{011}<2̄11>	(35,45,0)
Brass-Goss (auxiliary component)	B/G[1]	{011}<5̄11>	(20,45,0)
P-(B$_{ND}$) (auxiliary component)	P(B$_{ND}$)[2]	{011}<1̄11>	(47,45,0)
Copper Twin - II	Twin Cu - II	{233}<3̄11>	(23,50,56)
Brass-S (auxiliary component)	B/S[3]	{168}<2̄11>	(45,40,75)

1. B/G is an auxiliary component positioned between two commonly known ones, Bs and G.

2. P-(B_{ND}) is an auxiliary component related to a frequently occurring component Bs by a rotation around the normal direction.

3. B/S is the auxiliary component, which describes an intermediate scattering between the Bs and the S components.

4.2.5 Volume Fraction of the Texture Components

Cu Component

The volume fraction of the Cu component is quite high in pure Ni and Ni-Co alloys up to 40% Co additions. It is completely absent in Ni-60Co (Fig. 4.27). It is the most voluminous component in Ni-Co alloys upto Ni-30Co. But for Ni-40Co it is very low at 95% deformation. Thus Ni-40Co shows a transition in the Cu component before its complete disappearance in Ni-60Co.

S Component

The volume fraction of the S component shows a slight increasing tendency with deformation for alloys up to Ni-40Co, and for Ni-60Co a sharp increase in volume fraction is observed with increasing deformation (Fig. 4.27). Volume fraction of S component increases with Co additions only at high deformations in high Co content alloys (Fig. 4.28).

Bs Component

The volume fraction of Bs component shows contrasting trends in Ni-Co alloys up to Ni-40Co and in Ni-60Co. In pure Ni and Ni-Co alloys up to 40Co the volume fraction increases slightly with deformation (Fig. 4.27). But in Ni-60Co it decreases. All alloys up to Ni-30Co have very low volume fraction of Bs component which is less than 10%. In Ni-40Co too this component is only significant at 95% deformation. But for Ni-60Co the volume fraction of this component is always above 30%. Thus a predominant presence of Bs component is observed in Ni-60Co which decreases with deformation in this alloy.

B/G Component

This auxiliary component is present at a location intermediate between the Bs and G positions. It is present in all alloys at all deformations. It maintains an almost steady intensity in all alloys with deformation (Fig. 4.27). This component does not show any significant change with Co additions at any particular deformation level (Fig. 4.28).

Twin Cu-I Component

This component is completely absent in Ni-60Co, but is present in all the other cases. In the other cases it is only significant at beyond 90% deformation (Fig. 4.27). It doesn't seem to show any change with deformation or Co content (Fig. 4.28).

P(B_{ND}) Component

This component is present in pure Ni and Ni-Co alloys up to 40Co but only at lower deformations of 40 and 70% (Fig. 4.27). It is completely absent in Ni-60Co and does not show any variation in volume fraction with Co content (Fig. 4.28)or % deformation.

B/S Component

This component is completely absent in Ni-60Co. In pure Ni and all the rest Ni-Co alloys it shows significant volume fraction only at higher deformations (Fig. 4.27). No trends of change are visible with wt% Co at any particular deformation (Fig. 4.28).

Twin Cu-II Component

The twin Cu – II component {233}<311> is only present in Ni-60Co but absent in all Ni-Co alloys as well as pure Ni. The appearance of this component coincides with the disappearance of the Cu component and the twin Cu-I component in Ni-60Co (Fig. 4.27). The volume fraction of this component in Ni-60Co increases with deformation but registers a fall beyond 90% deformation.

G Component

The G component is present in all Ni-Co alloys with low volume fraction. It maintains almost constant volume fraction in Ni-Co alloys with deformation (Fig. 4.27). No trends are visible at a particular deformation with wt% Co (Fig. 4.28).

Random

The background or random includes the sum total of all the other orientations apart from those explicitly mentioned in the present work. In pure Ni the random component has almost 35% volume fraction at 90% deformation but at the other deformations it is almost zero. The random is significant in all other Ni-Co alloys up to 40%Co only at 70% deformation otherwise it is near to zero (Fig. 4.27). In Ni-60Co the random in all deformations is almost zero.

4.2.5 Intensities of the Texture Components

Cu Component

The Cu component shows a steady increase in intensity with deformation in pure Ni and alloys of 10,20 & 30Co(Fig. 4.29). A transition in the nature of the Cu component is observed for 40Co whence its intensity starts to decrease beyond 70% deformation leading to its complete absence in 60Co. Cu is the most intense component in all cases except in Ni-40Co 95% and Ni-60Co. At high deformations of 90 and 95% a fall in intensity of this component is only observed beyond Co additions of 30% (Fig. 4.30). Thus Ni-40%Co shows a transition of Cu component at high deformations of 90 and 95% leading to its complete absence in Ni-60Co.

Twin Cu - I Component

The twin Cu-I component makes its appearance in the various alloys only after 90% deformation. It is completely absent in Ni-60Co. This component shows increase in

intensity with deformation upto 30Co (Fig. 4.29), intensity slightly decreases in case of Ni-40Co beyond 90% deformation and it is completely absent in Ni-60Co. Thus twin Cu-I shows a transition with Co content. At any particular deformation this component does not show any change in intensity with Co addition (Fig. 4.30).

G Component

The G component shows constant intensity in all alloys irrespective of % deformation. The intensity values are very low for the G component (Fig. 4.29). For any particular deformation intensity of the G component is maximum in case of Ni-40Co (Fig. 4.30) and at 95% deformation it is maximum in Ni-60Co.

S Component

The S component shows a steady increase in intensity with deformation for all alloys upto Ni-40Co, but at Ni-60Co the intensity stays at a constant value and does not change with the degree of rolling (Fig. 4.29). Position wise the S component shows a considerable spread in Ni-60Co about the ideal orientation. At high deformation of 90 and 95% an intensity fall is observed beyond 30Co additions, same as that for the Cu component (Fig. 4.30).

Bs Component

The Bs component also registers an increase in intensity with deformation for alloys up to 40Co with major increase for higher deformations of 90 and 95% (Fig. 4.29). The intensity shows a marked increase from 40 to 60Co at any particular deformation (Fig. 4.30). Bs is the most intense component in Ni-60Co and in Ni-40Co at 95% deformation.

B/G Component

The B/G component shows almost constant intensity with deformation in the various alloys (Fig. 4.29). At any particular deformation it shows a slight increase in intensity with alloy additions upto Ni-40Co and then rises sharply to Ni-60Co (Fig. 4.30).

P(B$_{ND}$) Component

P(B$_{ND}$) is completely absent in Ni-60Co. In pure Ni it is present upto 90% deformation but in the other Ni-Co alloys it is only present till 70% deformation (Fig. 4.29). It maintains an intensity about 5 times randon in the various cases and does not show any trend of change with % deformation or wt% Co.

B/S Component

This component is absent in Ni-60Co. The intensity increases with deformation becoming as strong as the S and Bs components (Fig. 4.29). At particular deformation intensity of this component does not show any considerable variation with alloy additions up to 40%Co (Fig. 4.30).

Twin Cu II

This component is only present in Ni-60Co and increases in intensity with deformation (Fig. 4.29).

Figure 4.1   Micrographs taken from the longitudinal sections of pure Ni cold rolled at
(a) 40% (b) 70% (c) 90% and (d)95% deformations
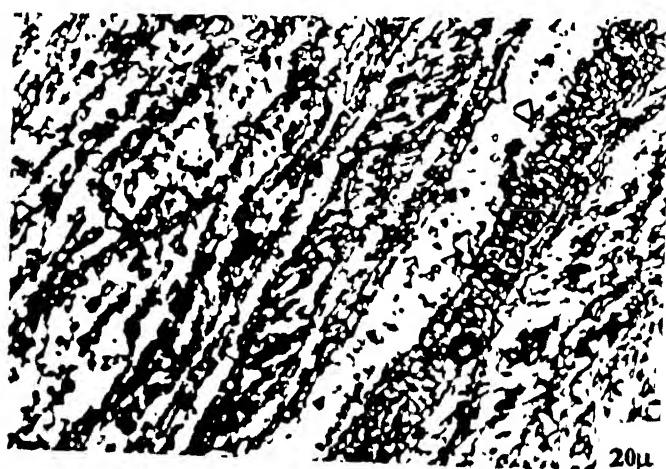
Figure 4.2   Micrographs taken from longitudinal sections of Ni-10Co (a) 40% cold
rolled (b) 70% cold rolled (c) 90% cold rolled and (d) 95% cold rolled

(a)

(b)

(c)

(d)

Figure 4.3   Micrographs taken from longitudinal sections of Ni-20Co (a) 40% cold
rolled (b) 70% cold rolled (c) 90% cold rolled and (d) 95% cold rolled
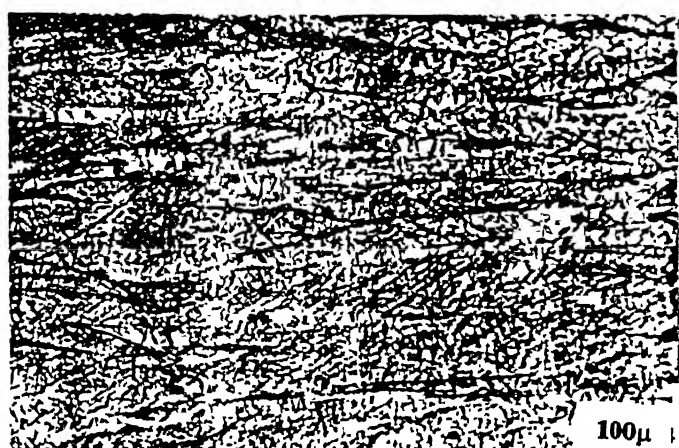
Figure 4.4   Micrographs taken from longitudinal sections of Ni-30Co (a) 40% cold
rolled (b) 70% cold rolled (c) 90% cold rolled and (d) 95% cold rolled
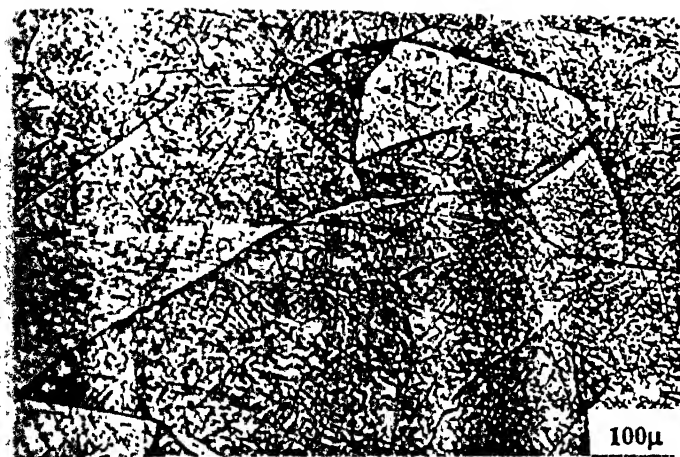
(a)

(b)

(c)

(d)

Figure 4.5   Micrographs taken from longitudinal sections of Ni-40Co (a) 40% cold
rolled (b) 70% cold rolled (c) 90% cold rolled and (d) 95% cold rolled

(a)

(b)

(c)
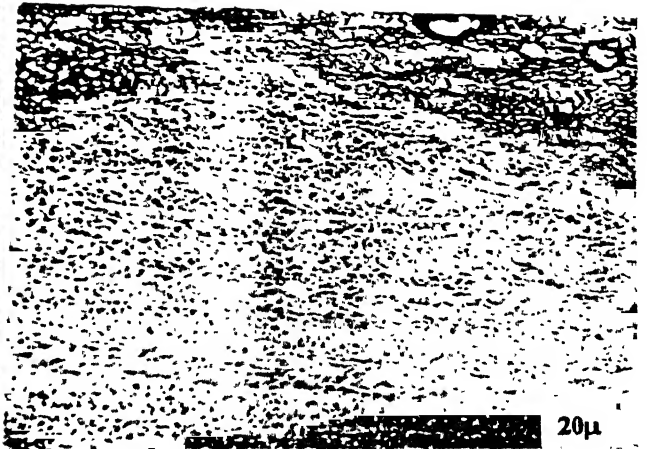
(d)

Figure 4.6   Micrographs taken from longitudinal sections of Ni-60Co (a) 40% cold
rolled (b) 70% cold rolled (c) 90% cold rolled and (d) 95% cold rolled
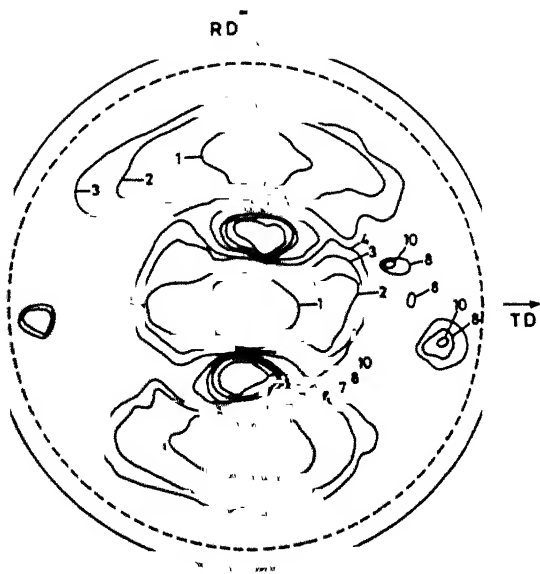
Pure Ni 40% CW
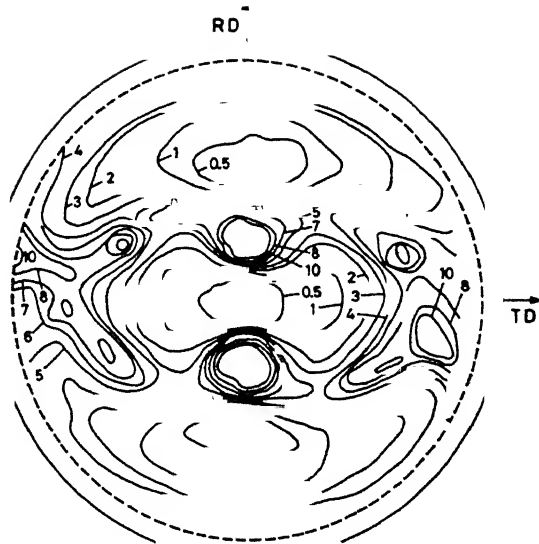
Pure Ni 70% CW
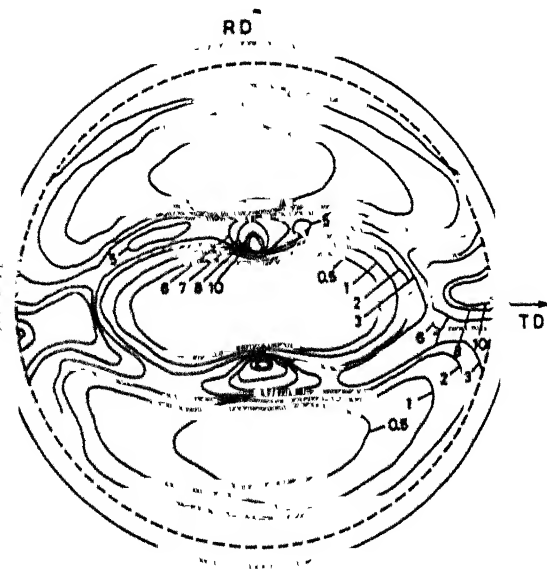
Pure Ni 90% CW
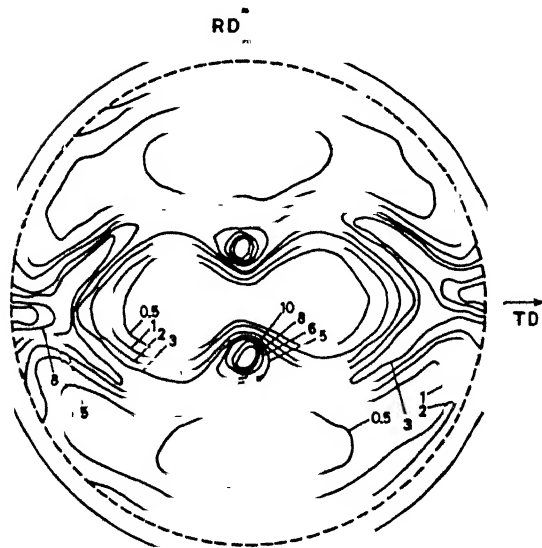
Pure Ni 95% CW

Figure 4.7 {111} pole figures showing the cold rolling textures developed in Pure Ni
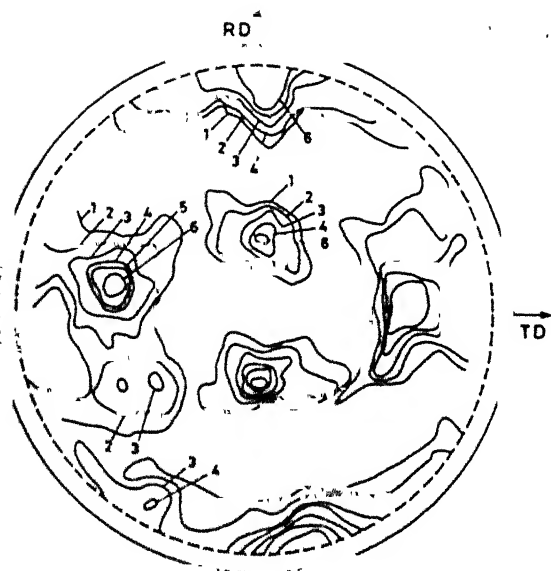
Ni-10Co 40% CW
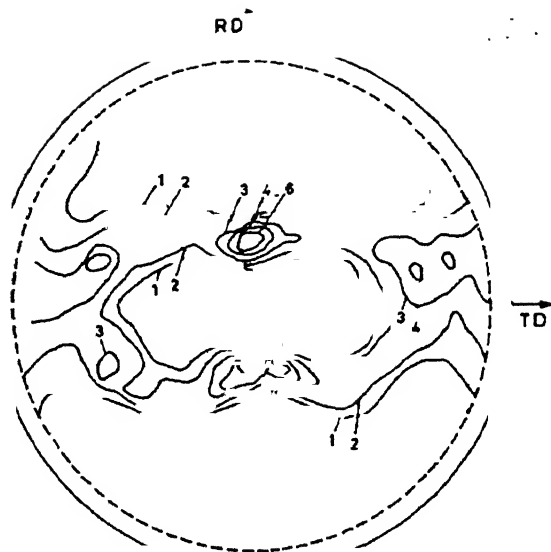
Ni-10Co 70% CW
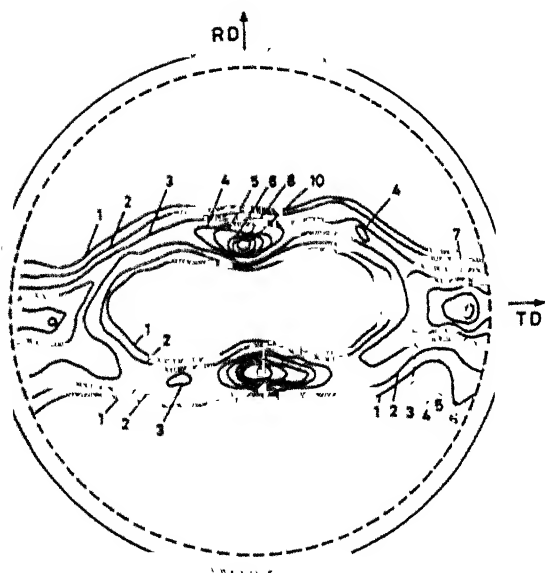
Ni-10Co 90% CW
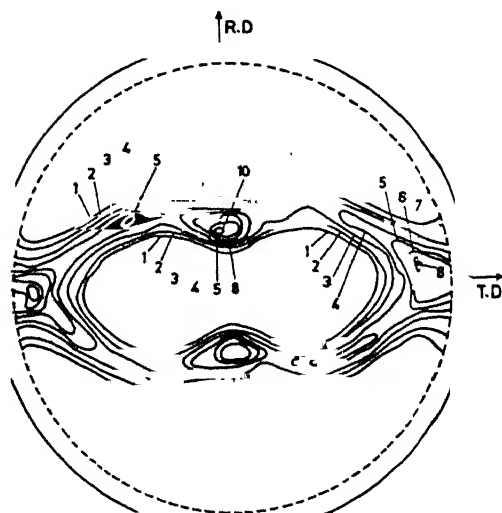
Ni-10Co 95% CW

Figure   4.8   {111} pole figures showing the cold rolling textures developed in Ni-10%Co
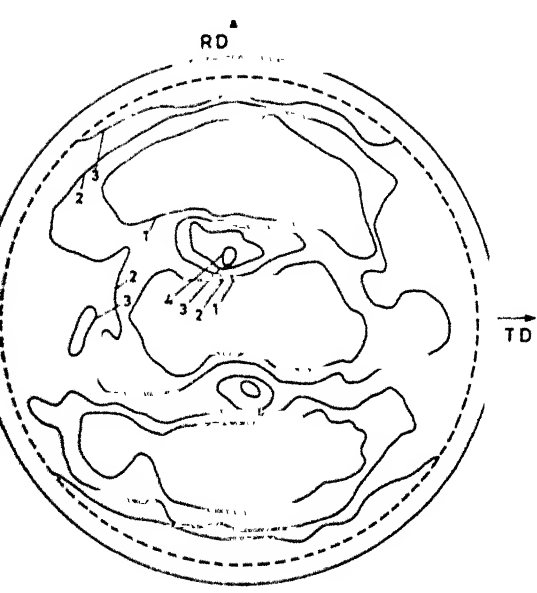
Ni-20Co 40% CW
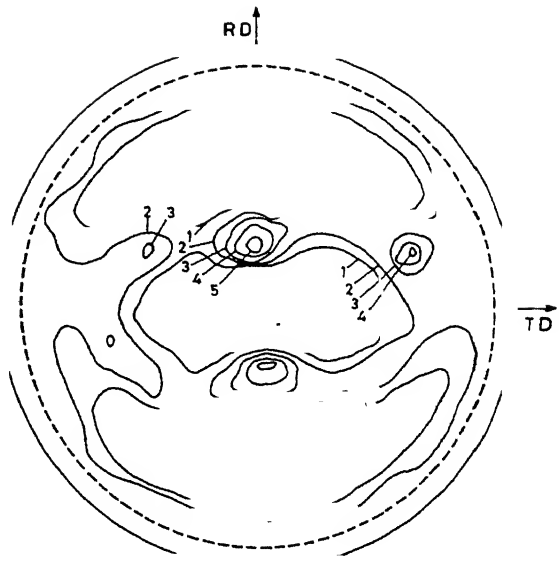
Ni-20Co 70% CW
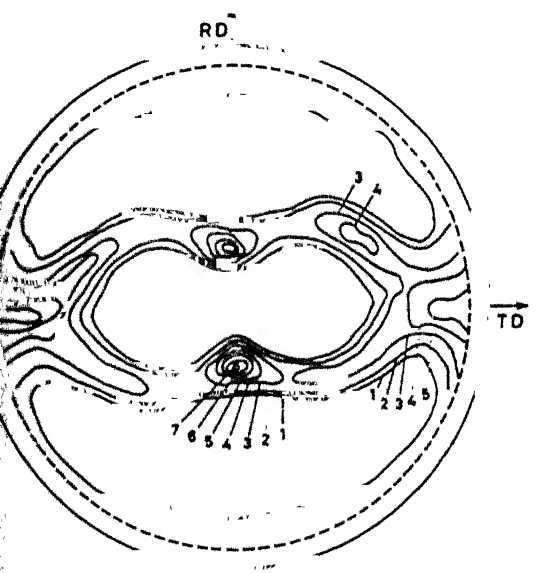
Ni-20Co 90% CW
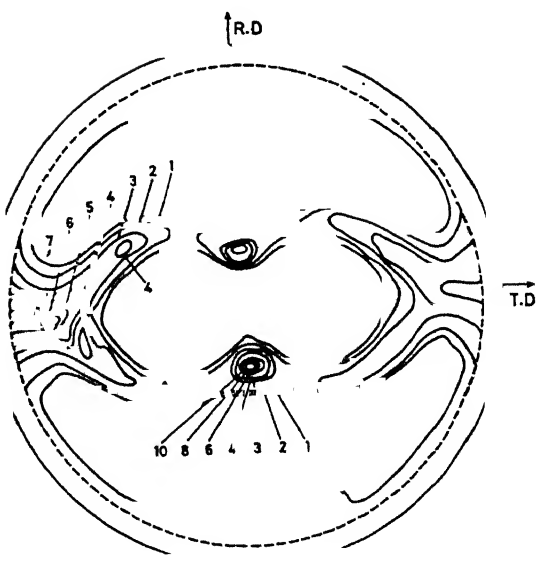
Ni-20Co 95% CW

Figure 4.9 {111} pole figures showing the cold rolling textures developed in Ni-20%Co

Ni-30Co 40% CW

Ni-30Co 70% CW

Ni-30Co 90% CW
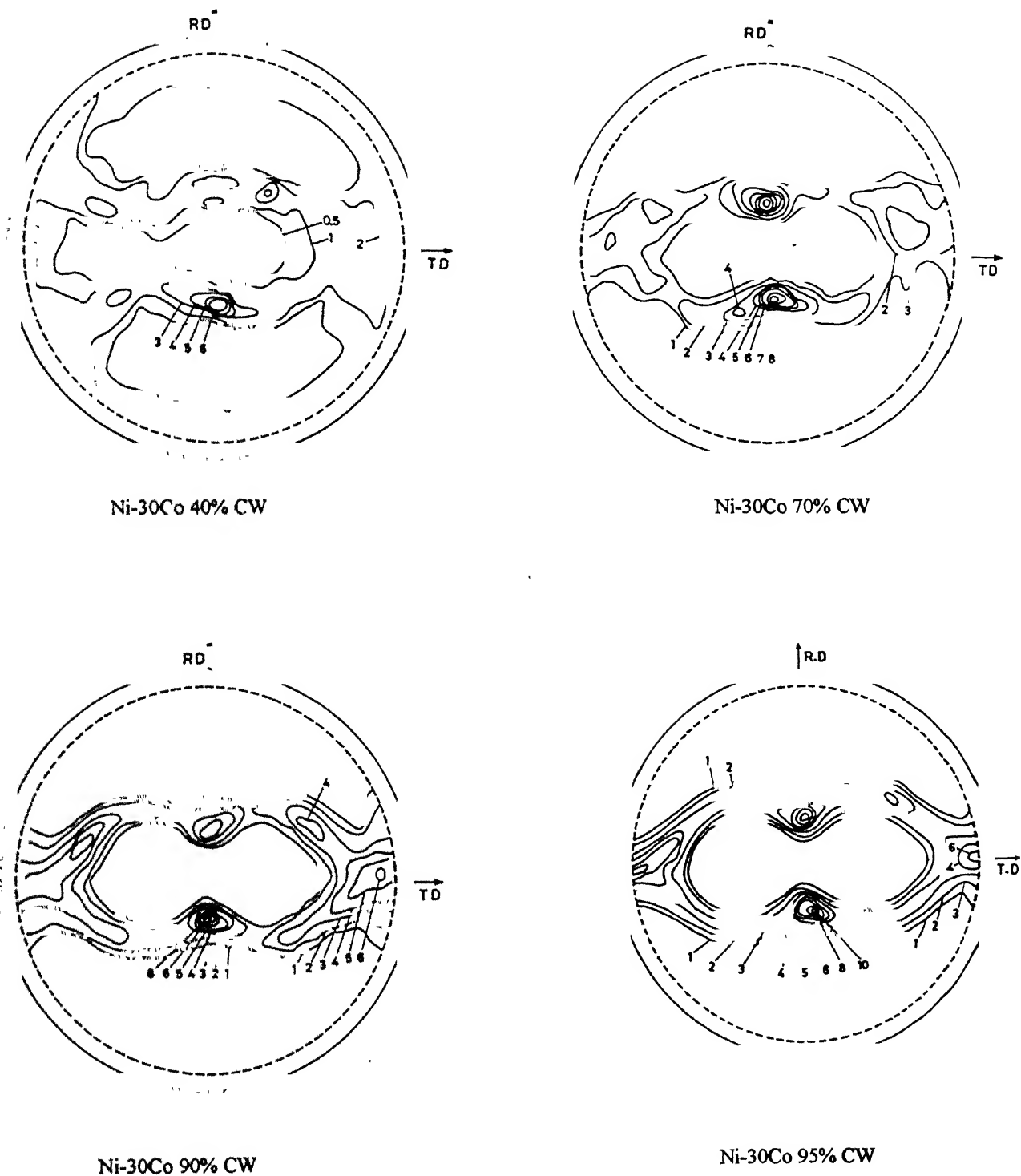
Ni-30Co 95% CW

Figure 4.10   {111} pole figures showing the cold rolling textures developed in Ni-30%Co

Ni-40Co 40% CW

Ni-40Co 70% CW

Ni-40Co 90% CW
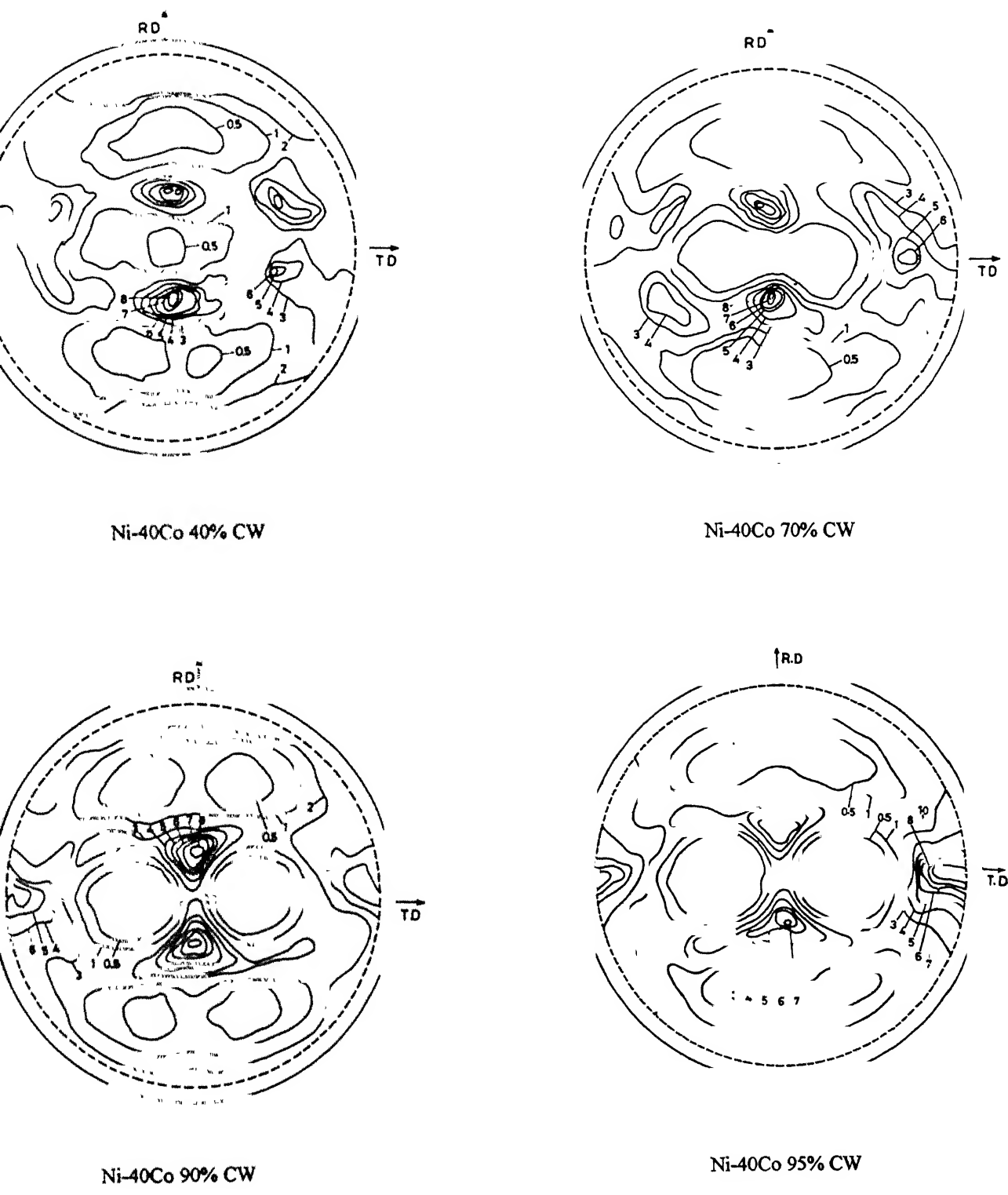
Ni-40Co 95% CW

Figure 4.11   {111} pole figures showing the cold rolling textures developed in Ni-40%Co
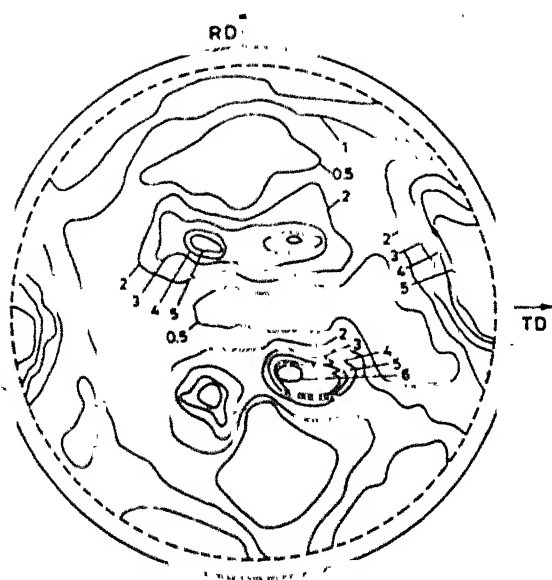
Ni – 60Co 40%CW
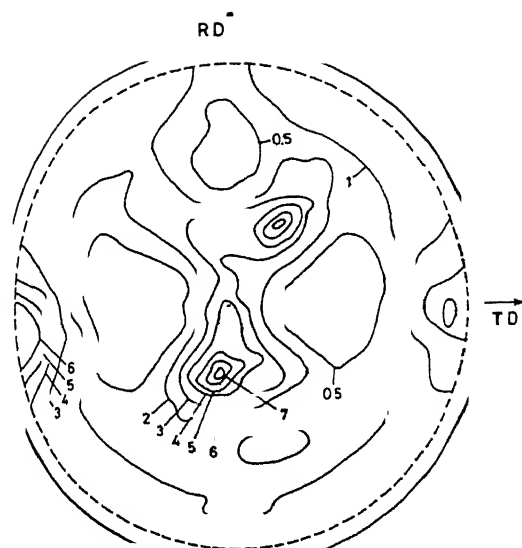
Ni – 60Co 70%CW
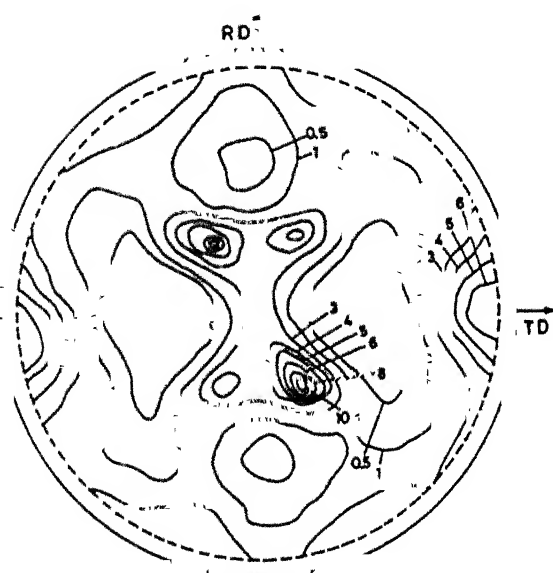
Ni – 60Co 90% CW
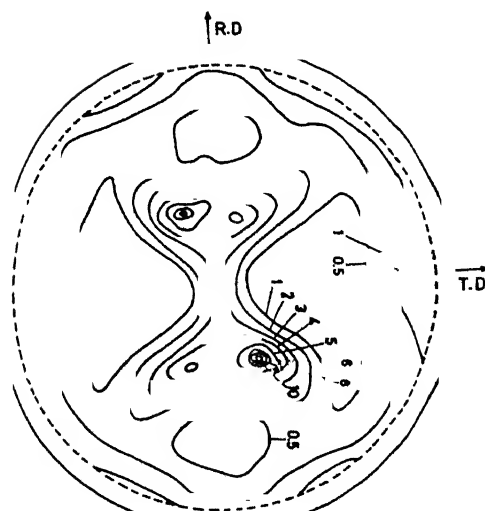
Ni – 60Co 95%CW

ure 4.12   {111} pole figures showing the cold rolling textures developed in Ni-60%Co
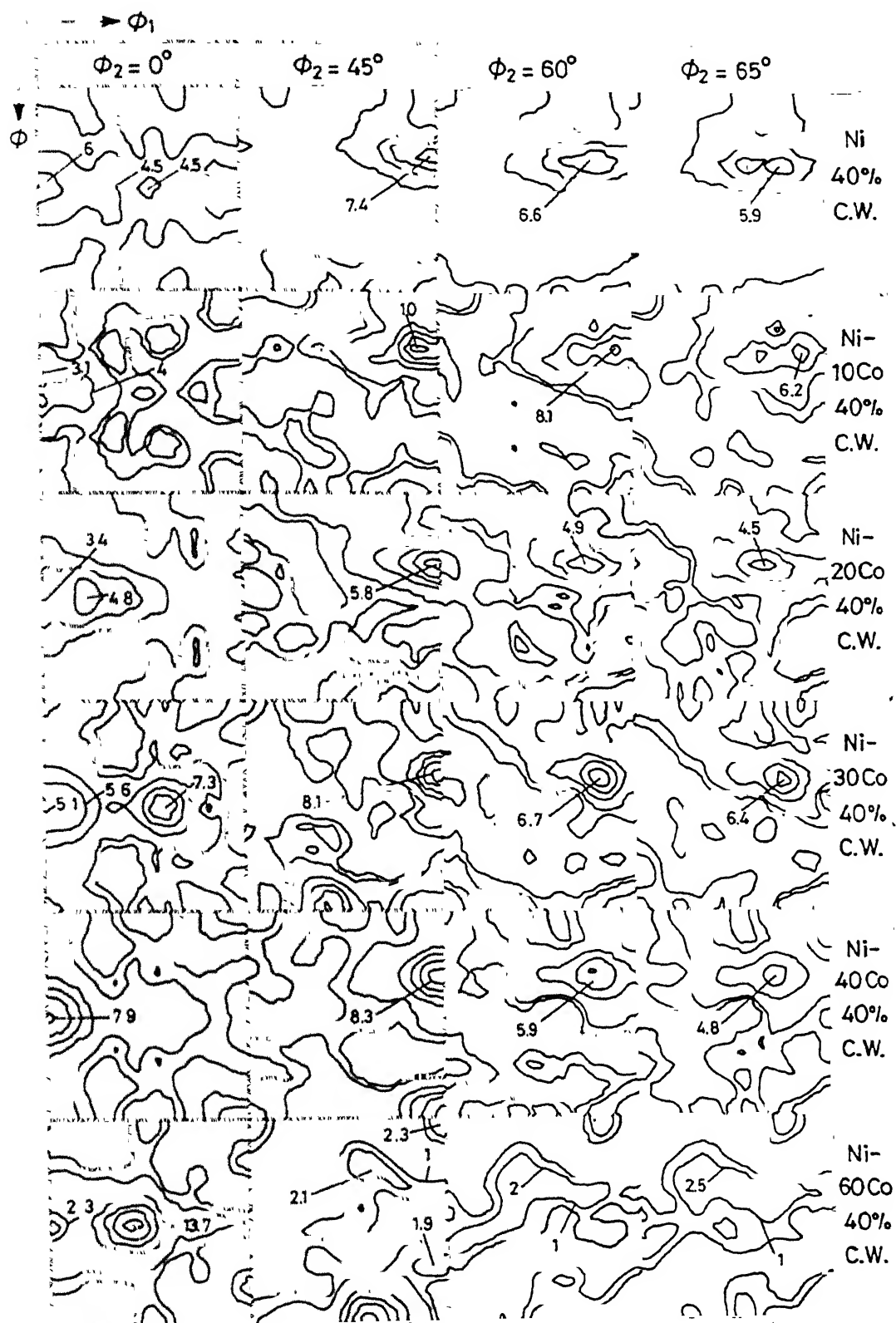
Figure 4.13   Sections of the O.D.F.s for 40% cold rolled pure Ni and the Ni-Co alloys.
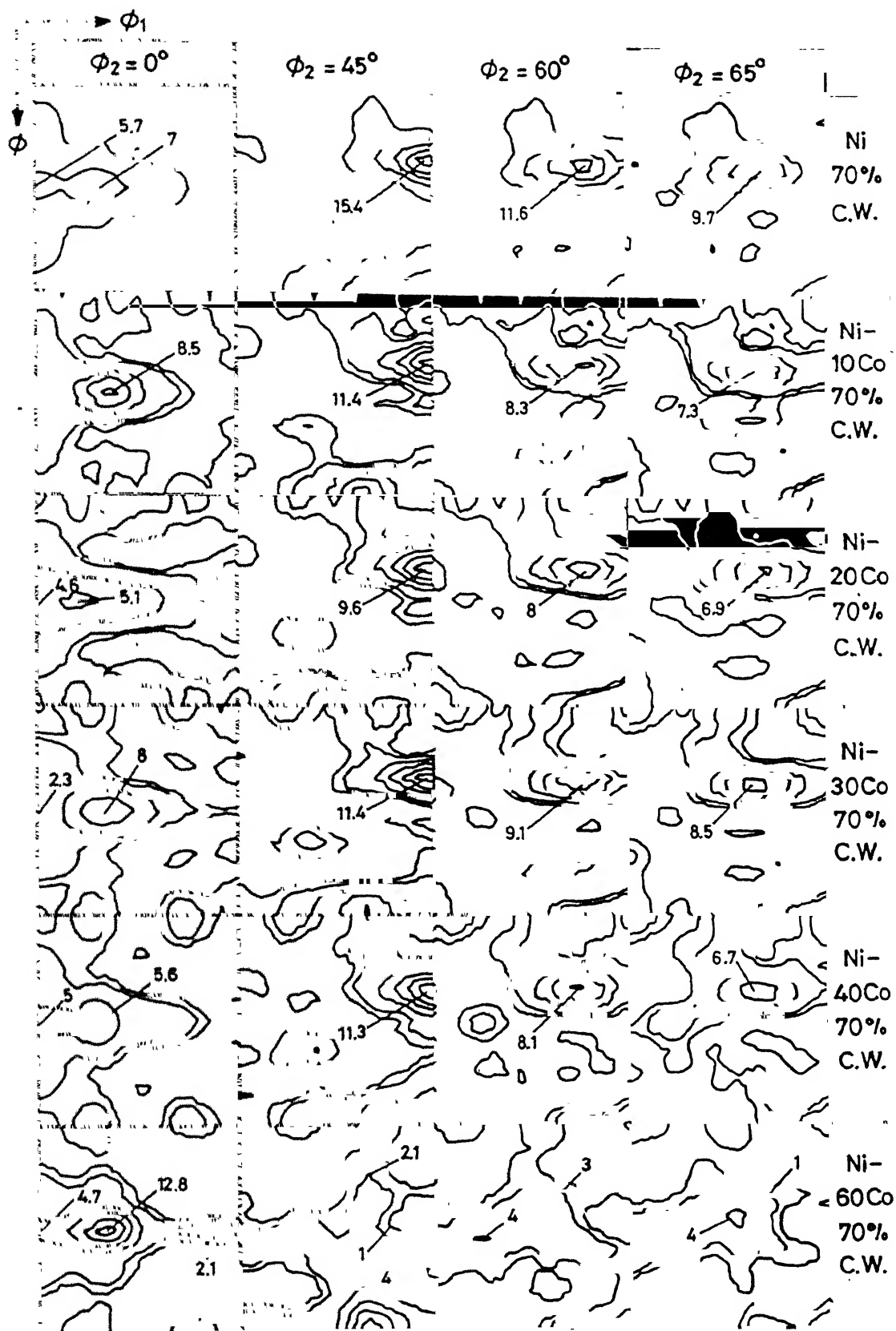
Figure 4.14.   Sections of the O.D.F.s for 70% cold rolled pure Ni and the Ni-Co alloys
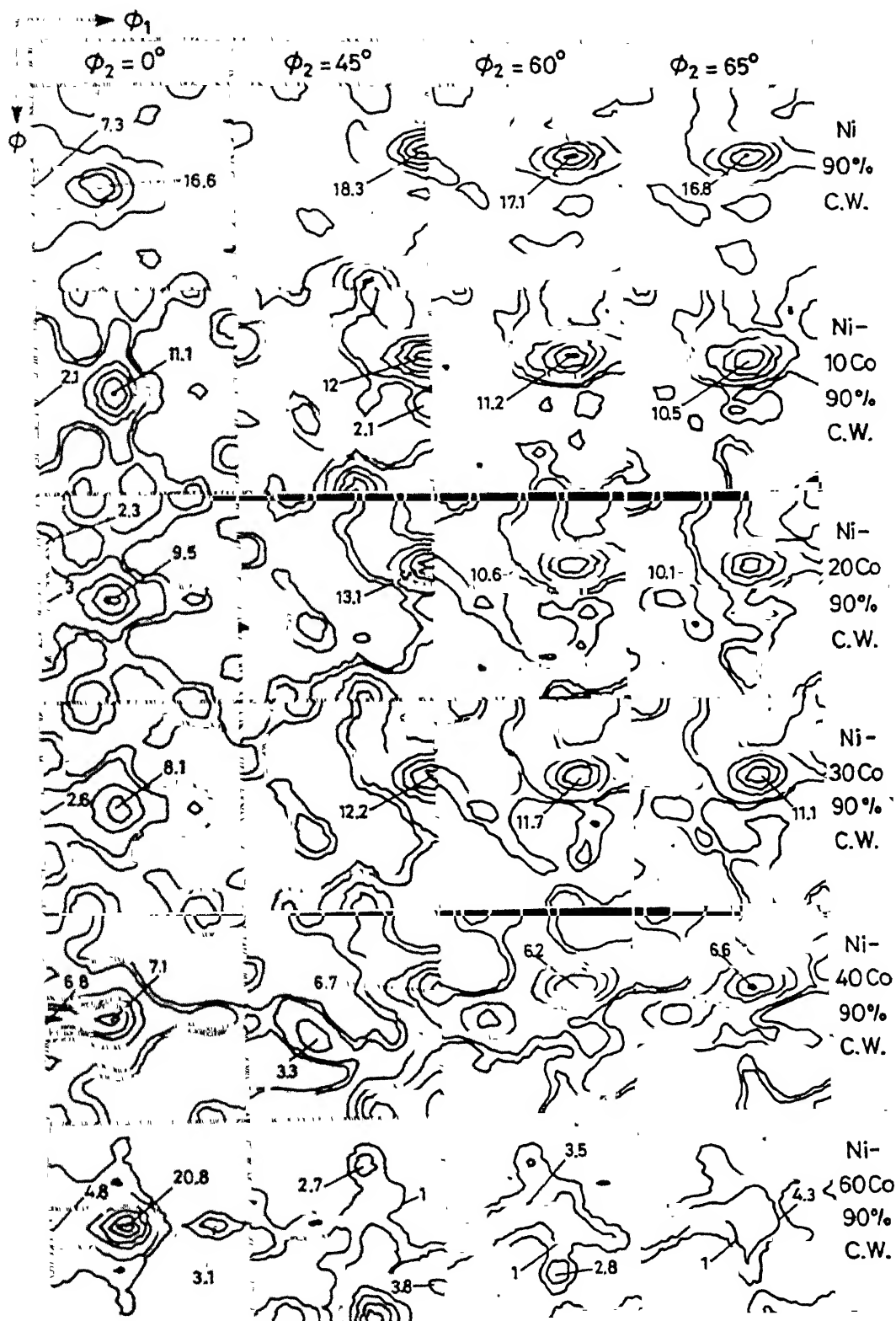
Figure 4.15 Sections of the O.D.F.s for 90% cold rolled pure Ni and the Ni-Co alloys.
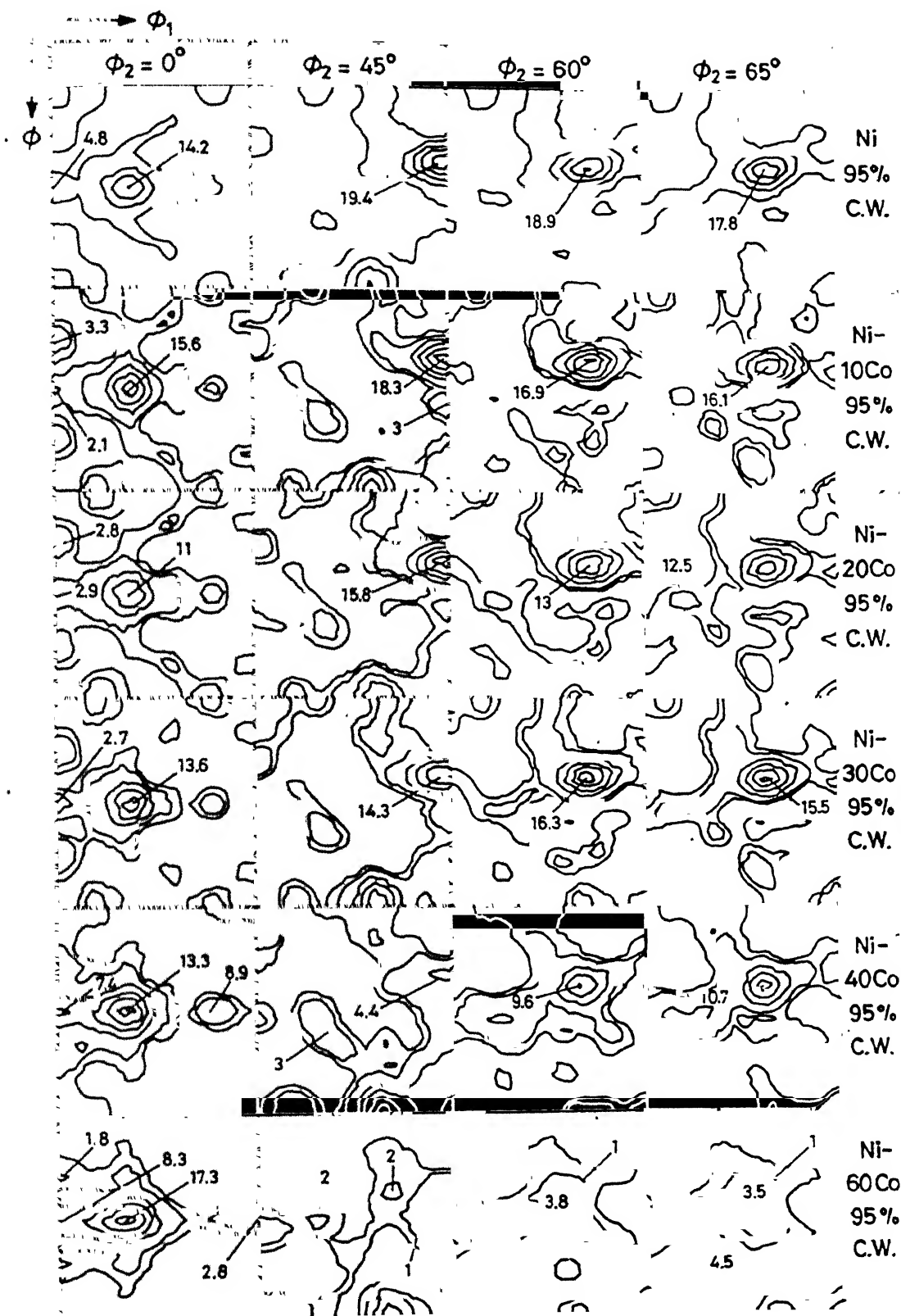
Figure 4.16   Sections of the O.D.F.s for 95% cold rolled pure Ni and the Ni-Co alloys.
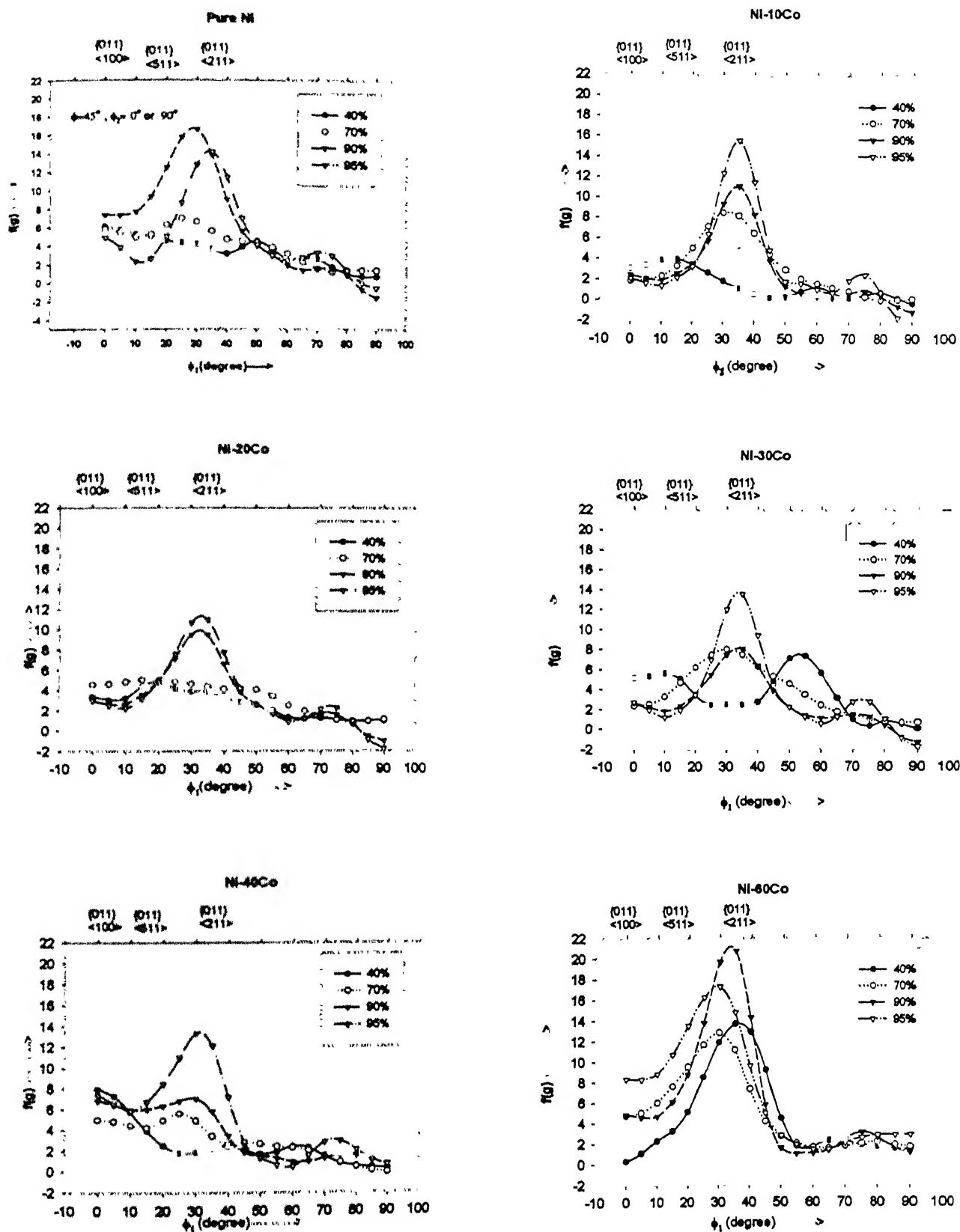
Figure 4.18   Plots of f(g) vs ϕ_1(α fibre) along the line $\phi = 45^0$, $\phi_2 = 0^0$ or 90^0, Ni-Co alloys at various
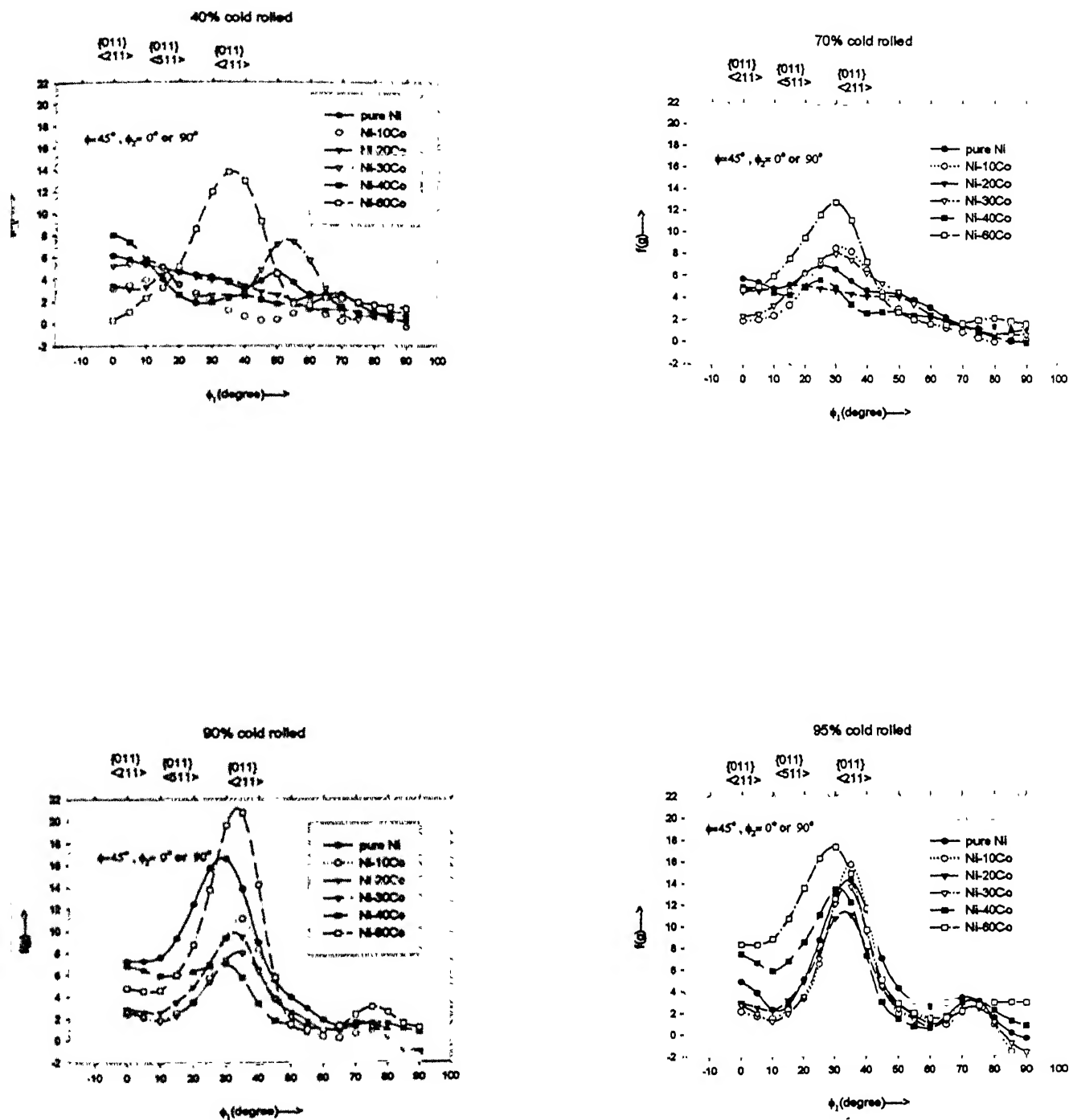
Figure 4.19   Plots of f(g) vs ϕ_1(α fibre) along the line $\phi = 45^0$, $\phi_2 = 0^0$ or 90^0, at particular

Pure Ni
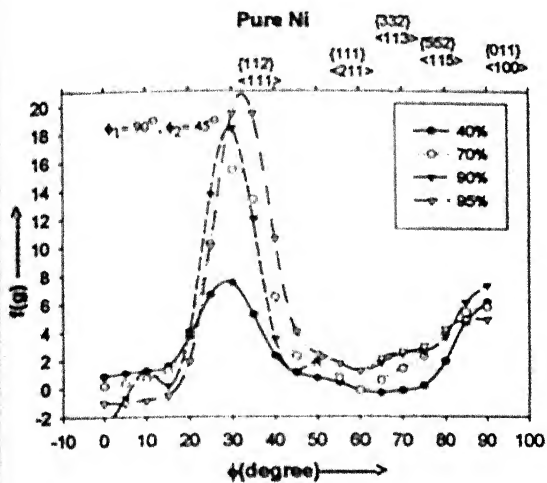
Ni-10Co
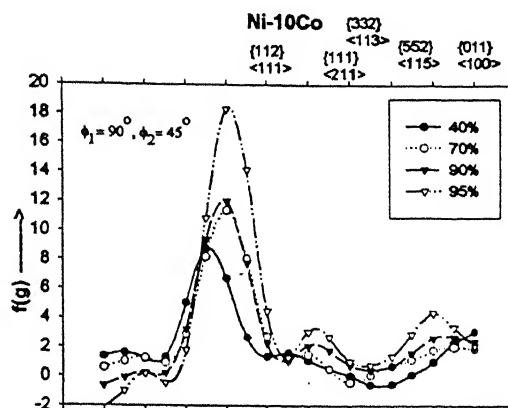
Ni-20Co
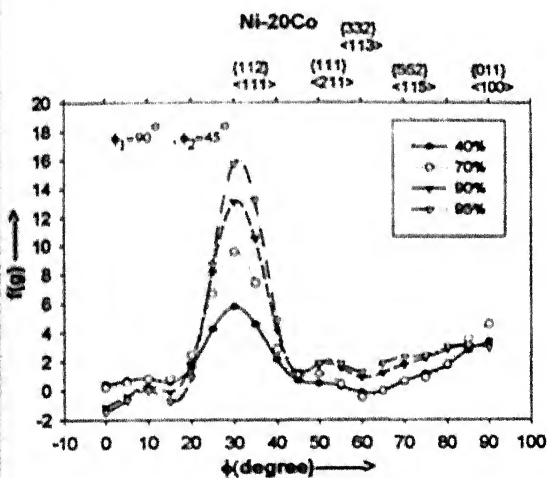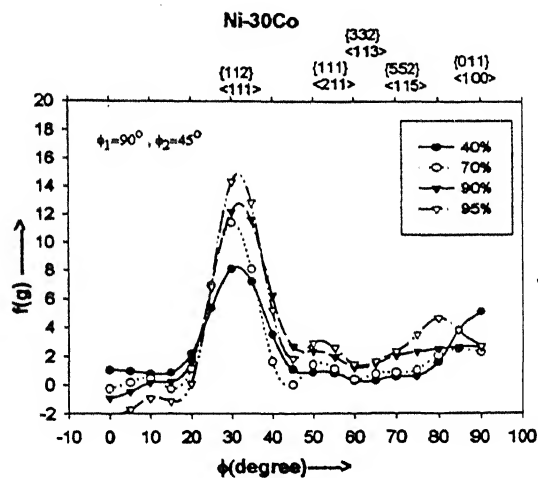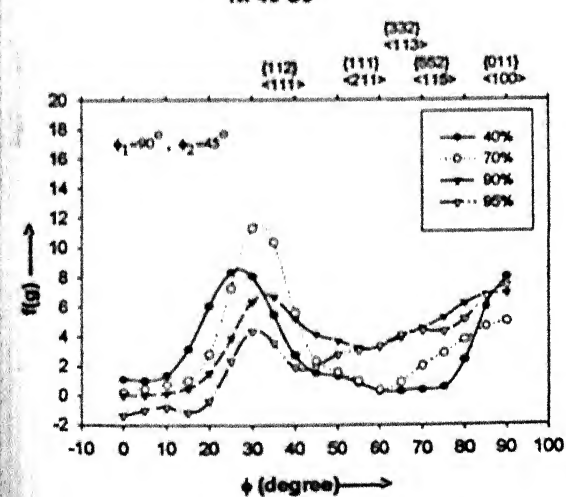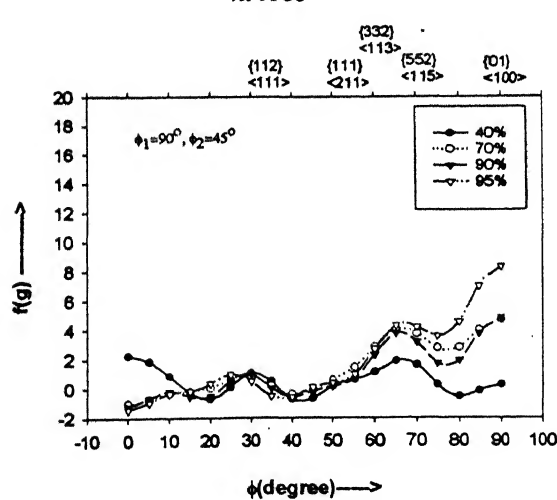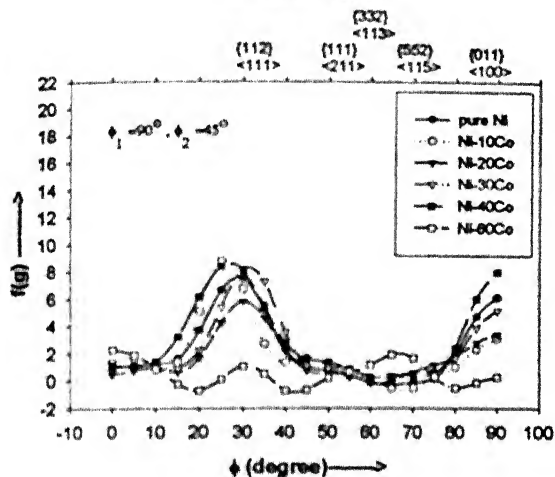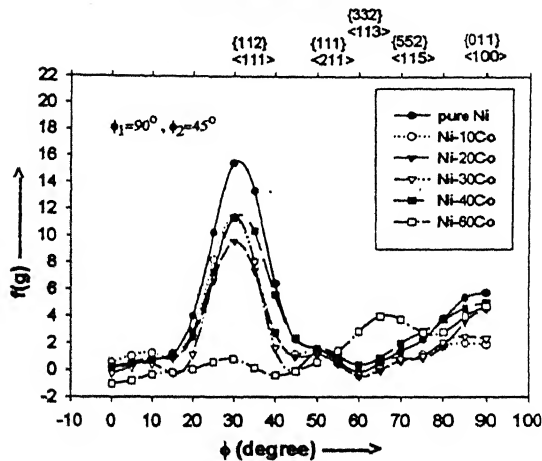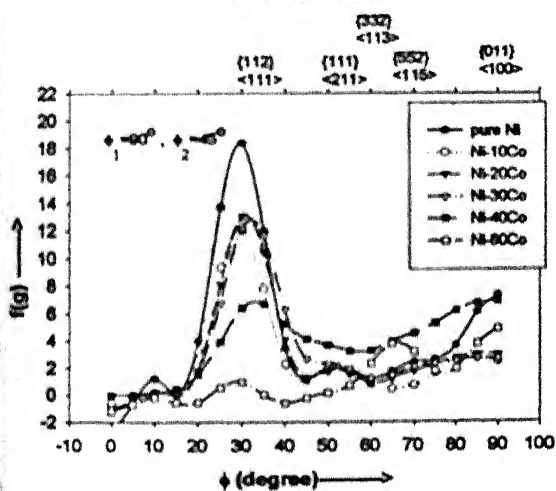
Ni-30Co
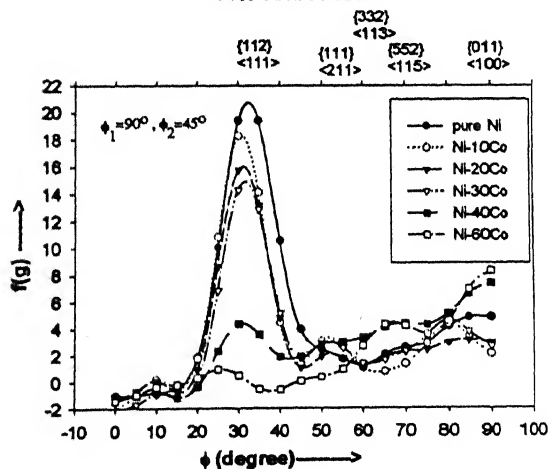
Ni-40 Co

Ni-60Co

Figure 4.21   Plots of f(g) vs φ(τ fibre) along the line φ₁ = 90⁰, φ₂ = 45⁰, at particular
deformations for different Ni-Co alloys.

Pure Ni
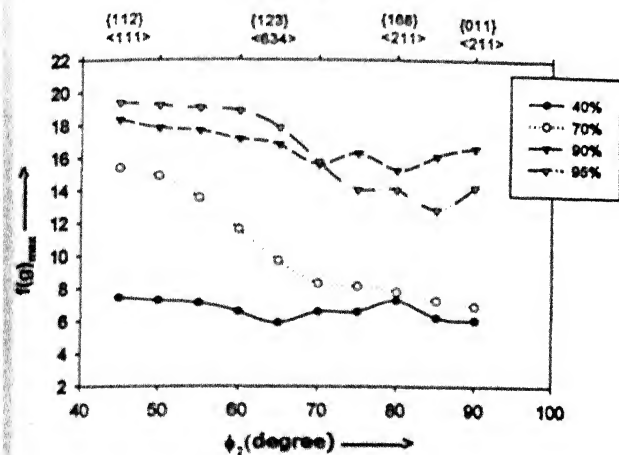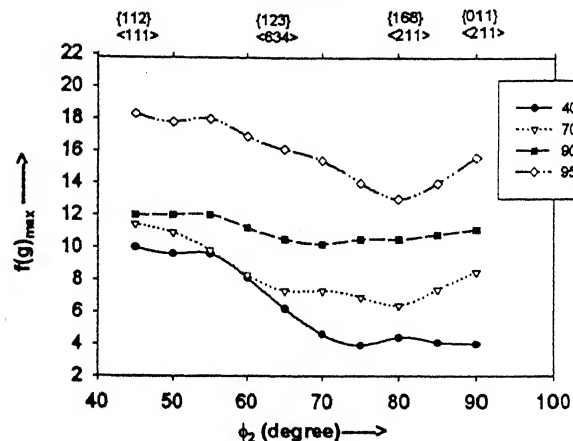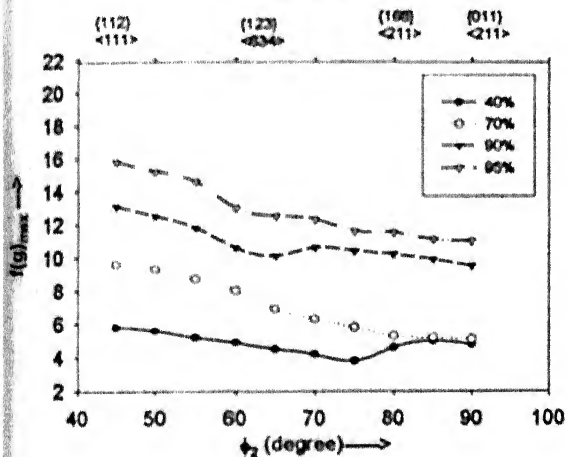
Ni-10Co

Ni-20Co

Ni-30Co
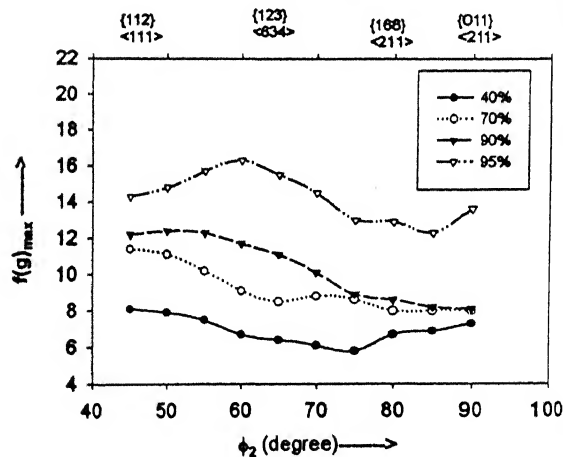
Ni-40Co
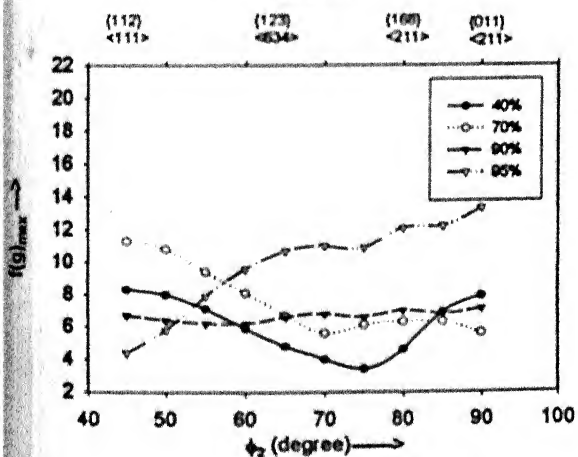
Ni-60Co
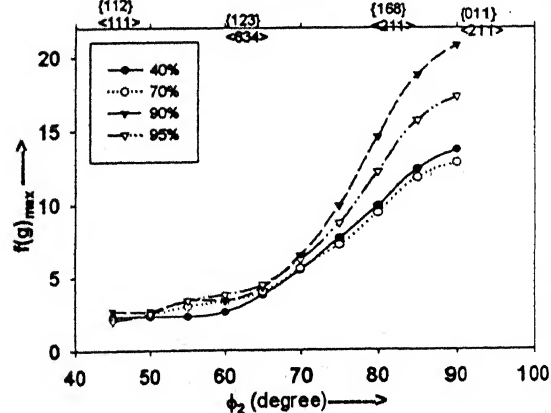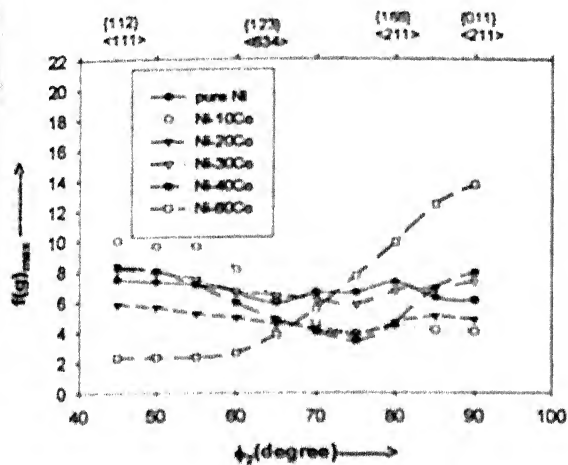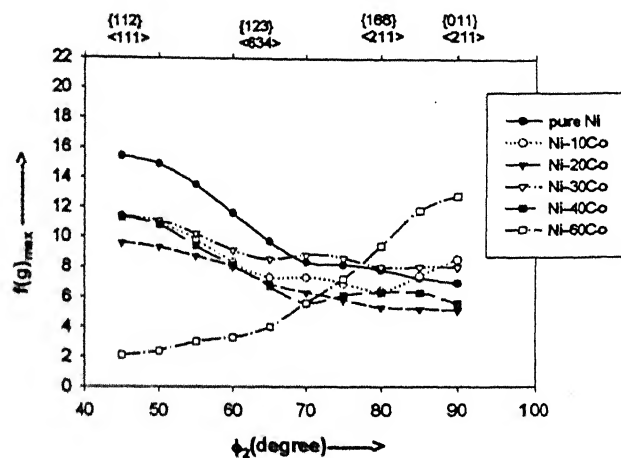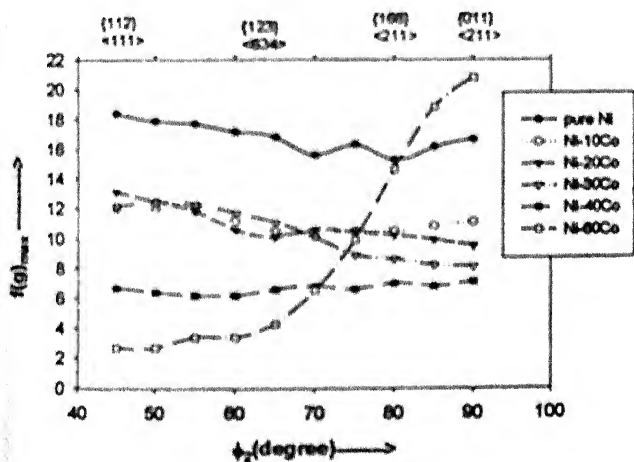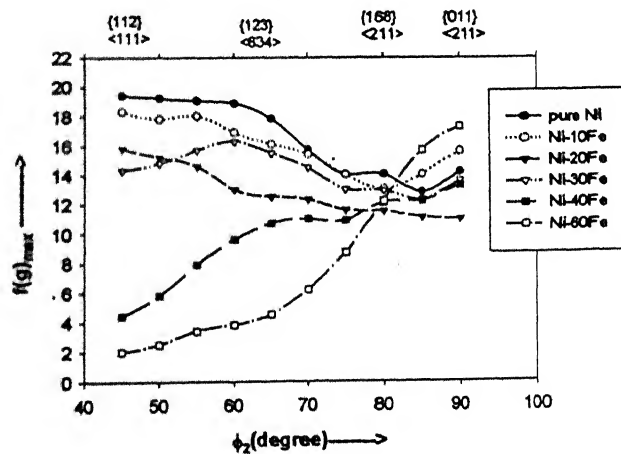
Figure 4.23   Plots of f(g)$_{max}$ vs ϕ_2 (β fibre) at a particular deformation for various Ni-Co alloys.

PURE Ni

Ni-10Co

Ni-20Co

Ni-30Co

Ni-40Co

Ni-60Co
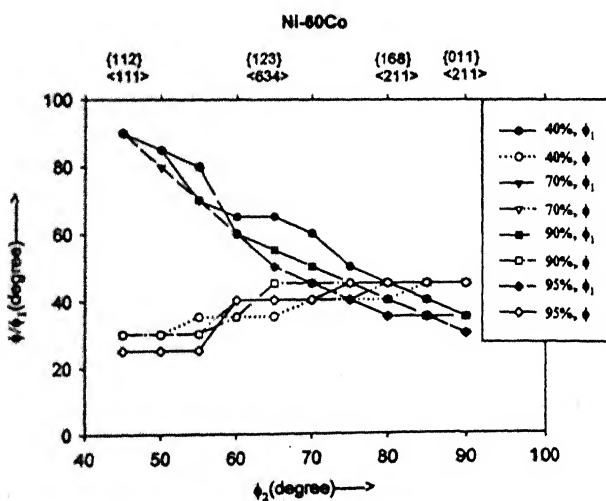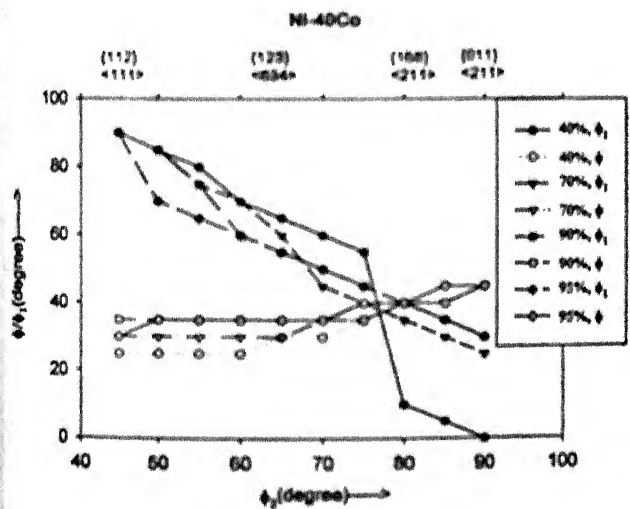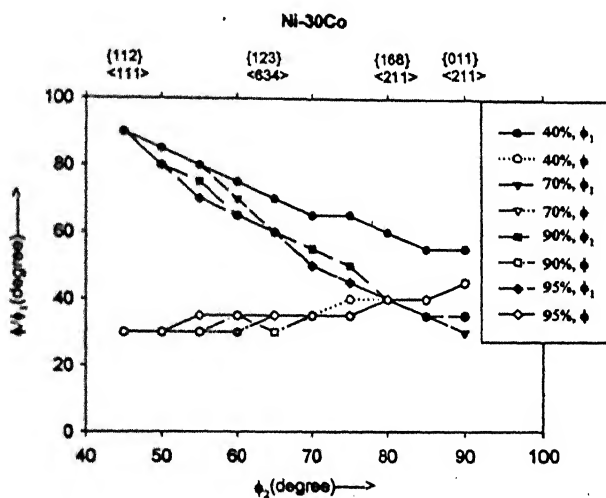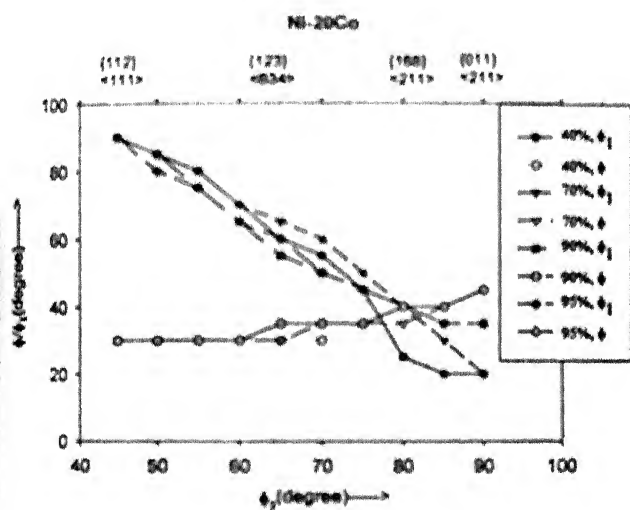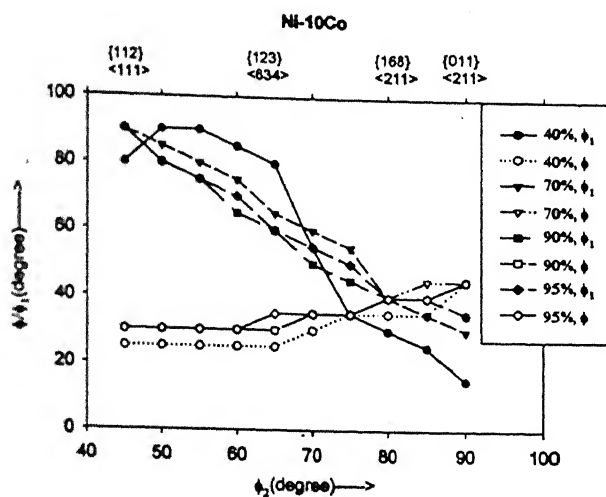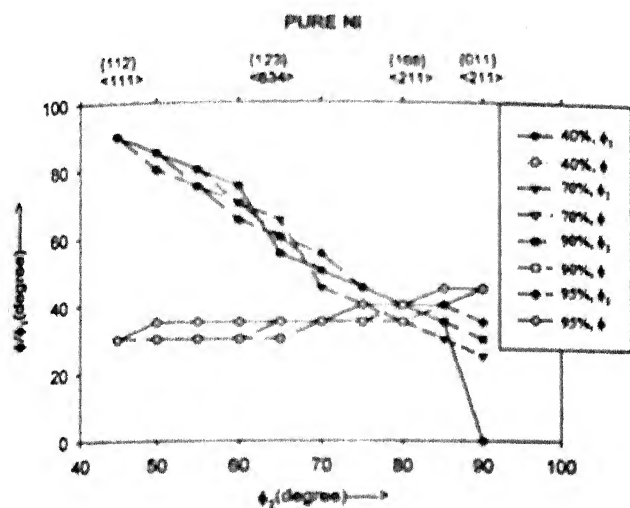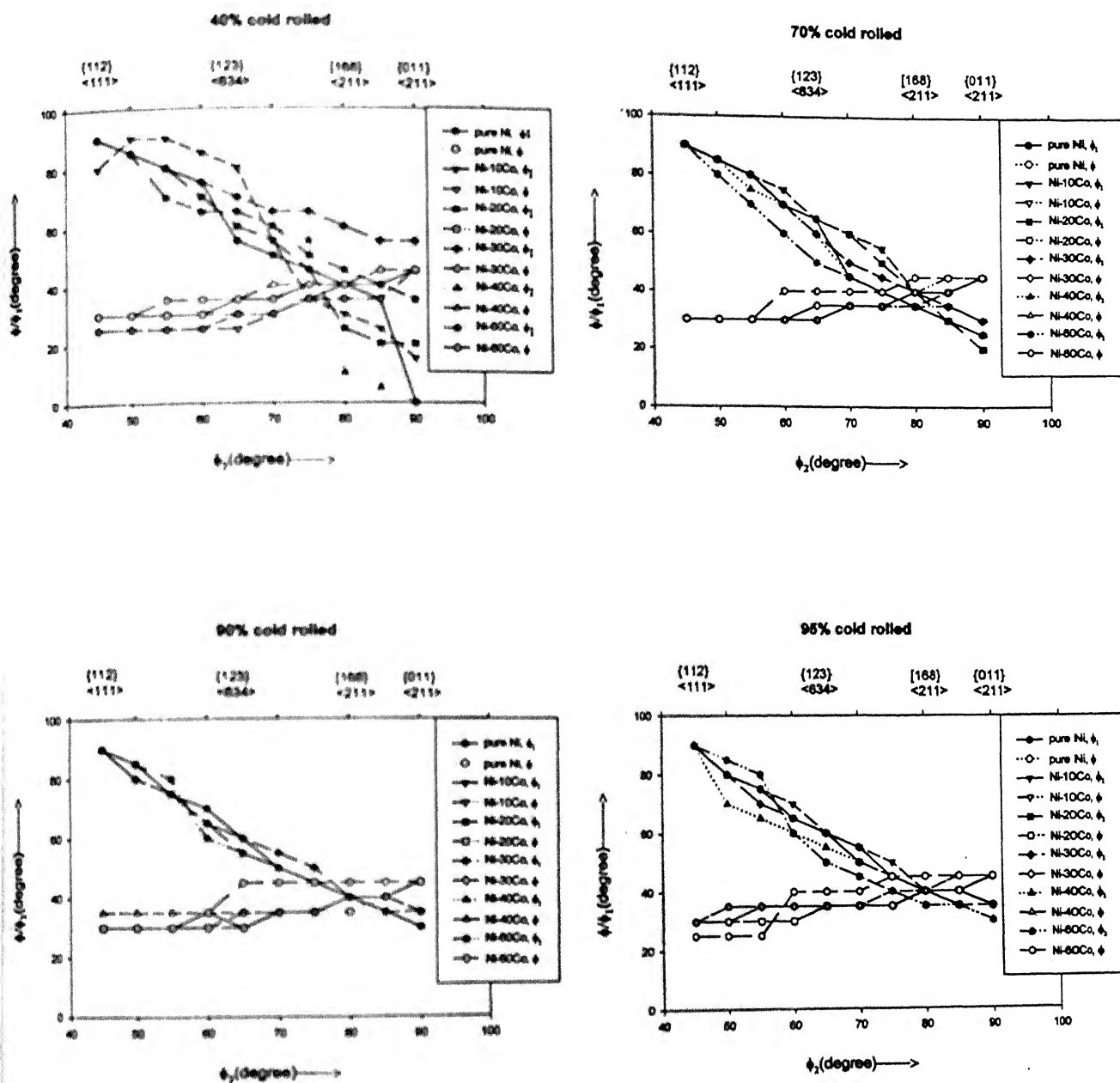
Figure 4.25　　Plots showing the course of the β fibre at a particular deformation in the various Ni-Co alloys.
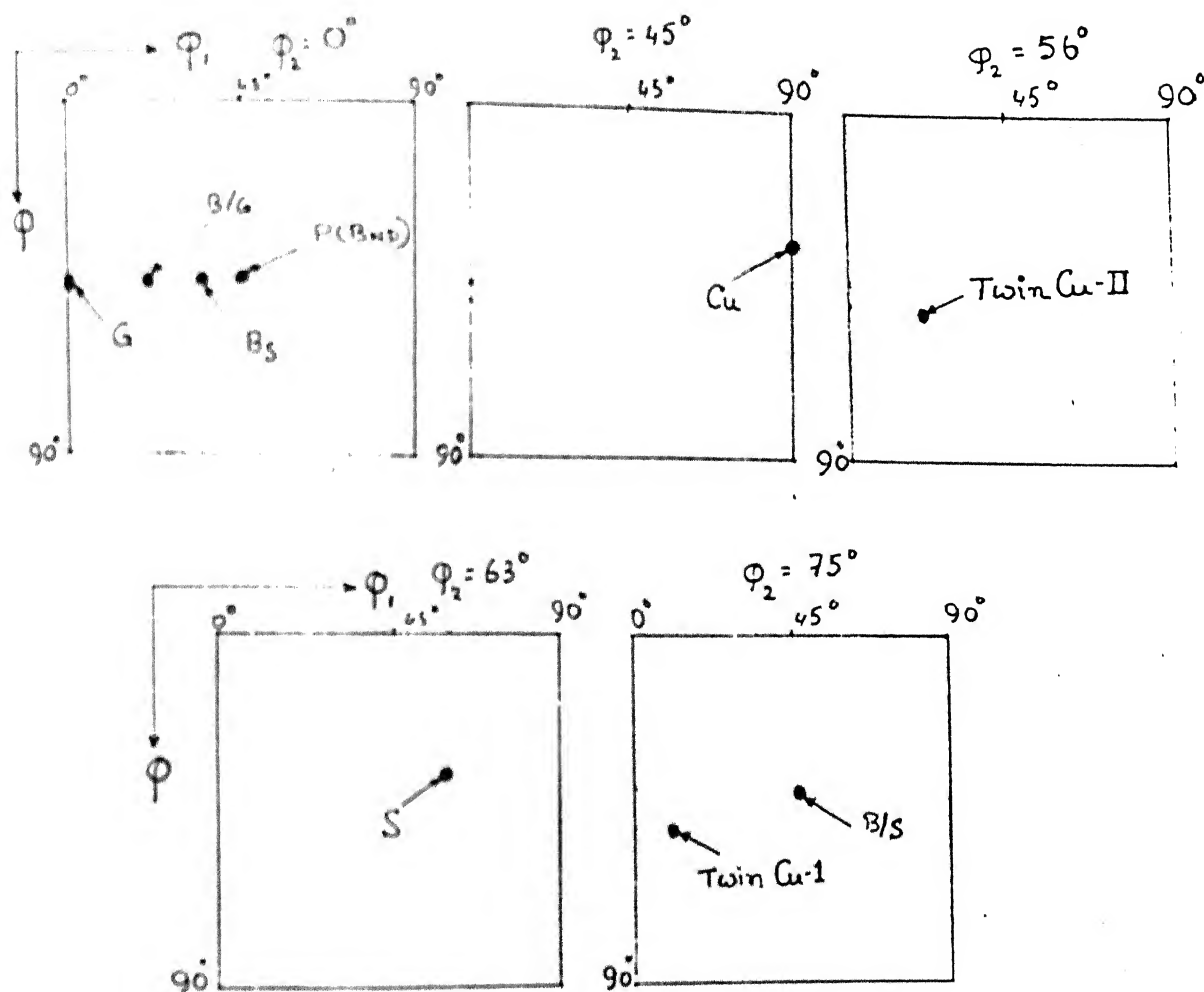
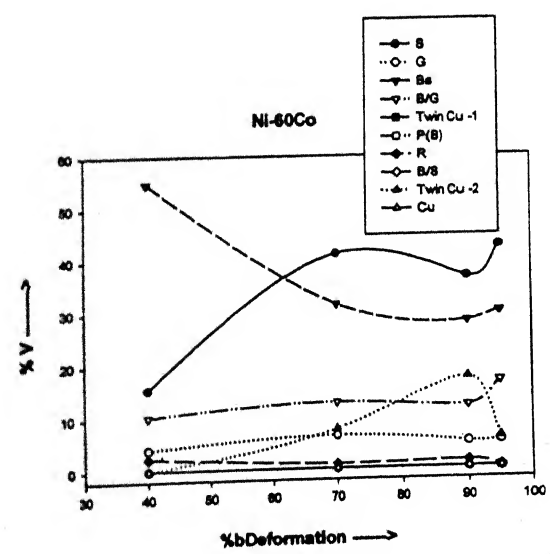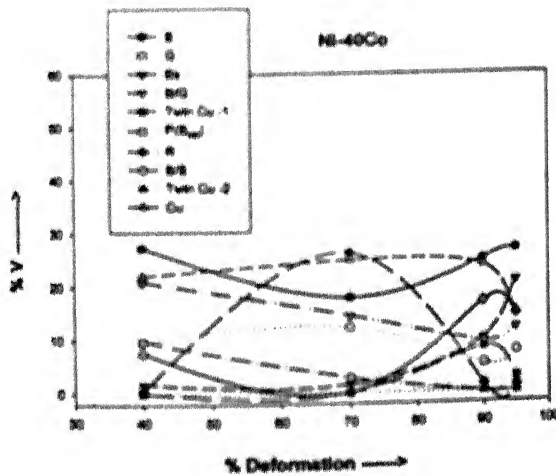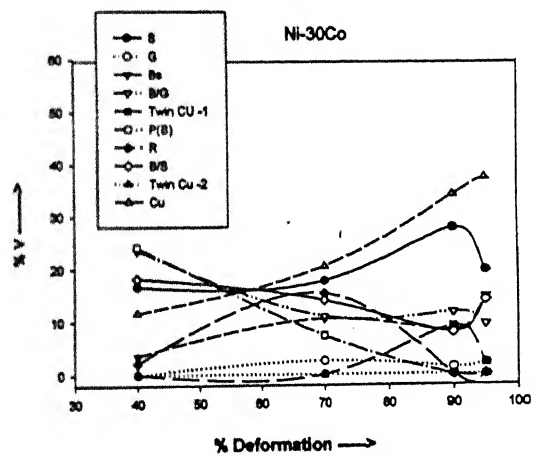Fig 4.26   Position of the various texture components identified in Ni-Co alloys in the relevant ϕ_2 sections of Euler space.
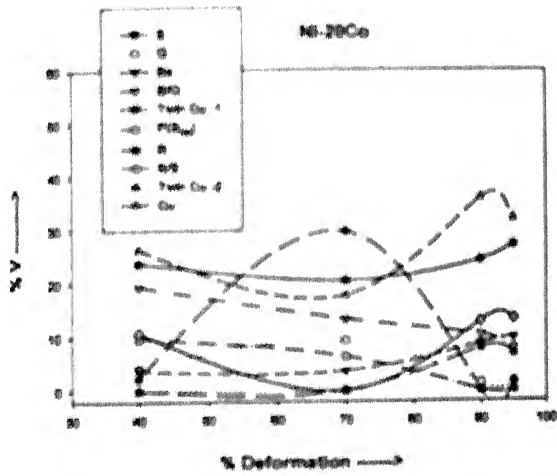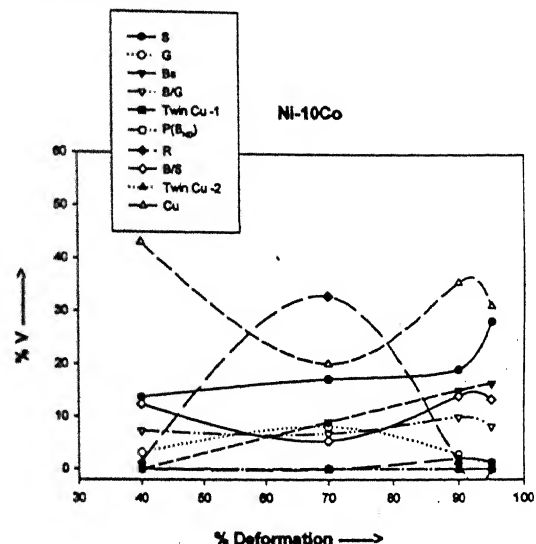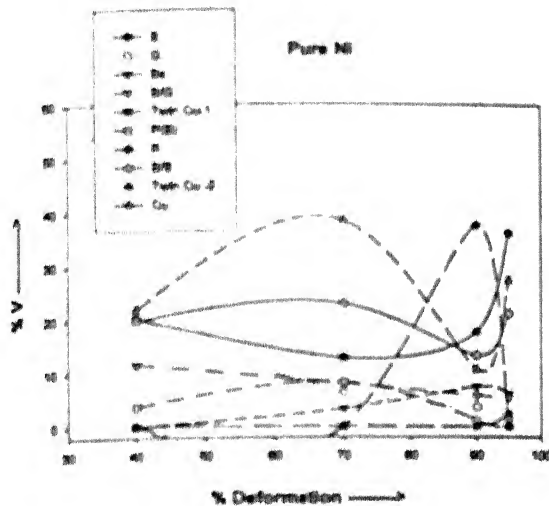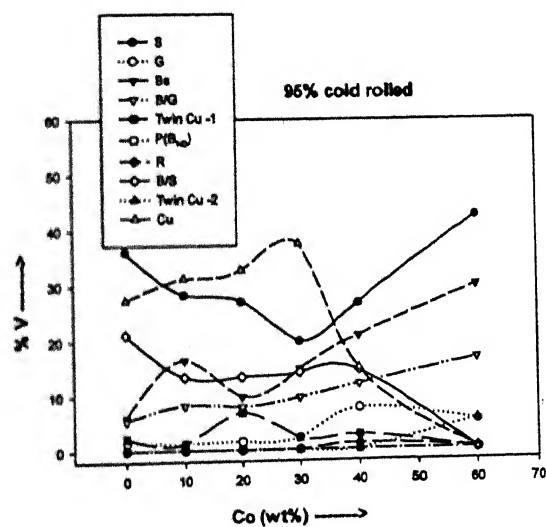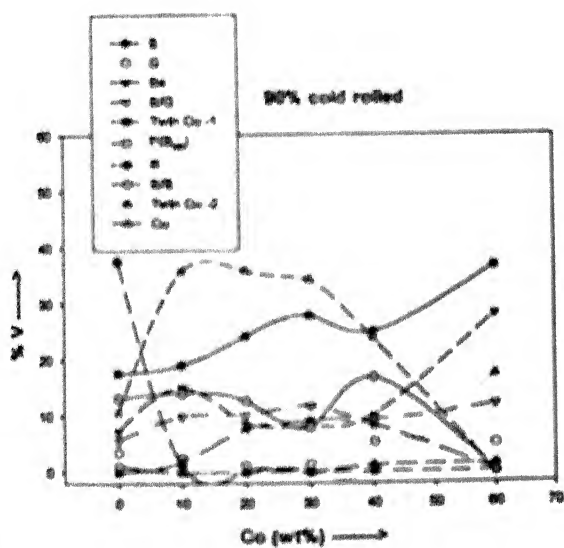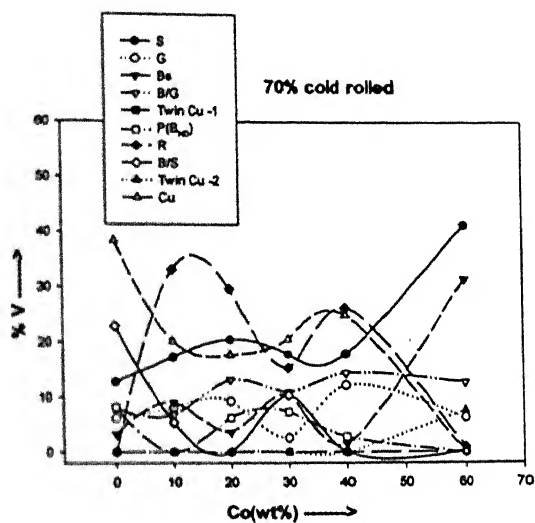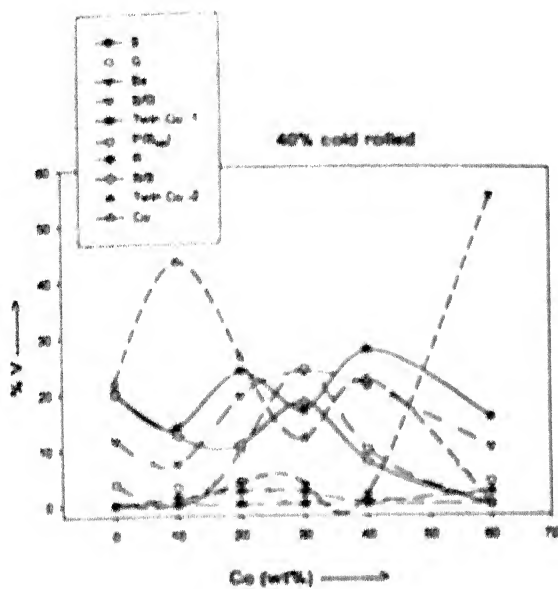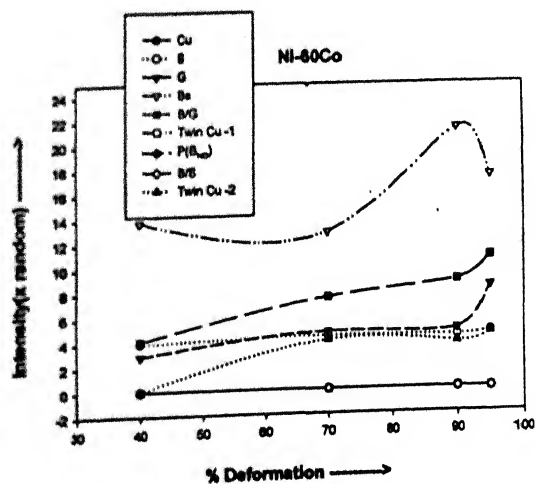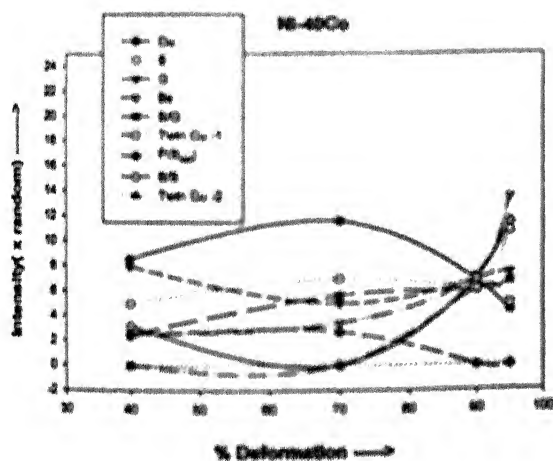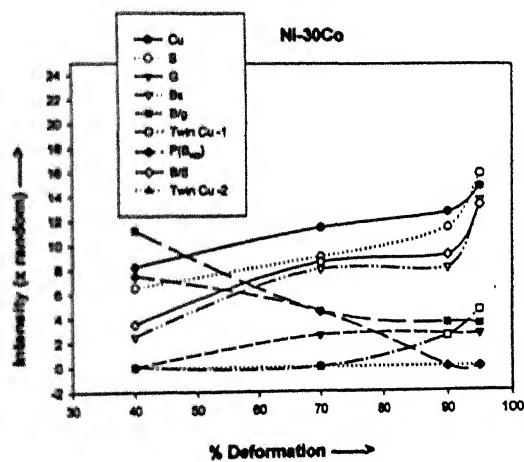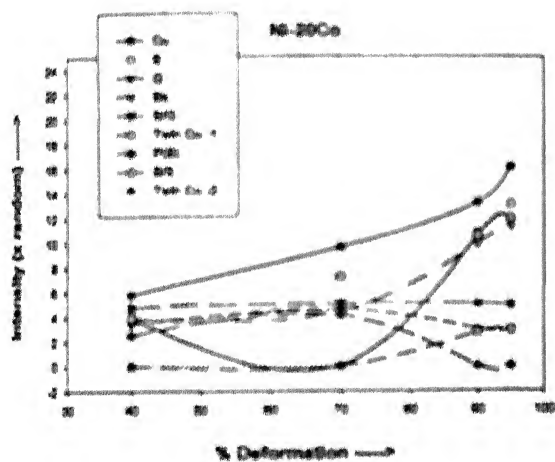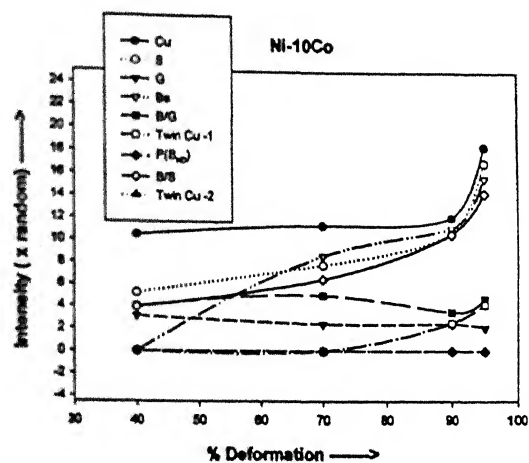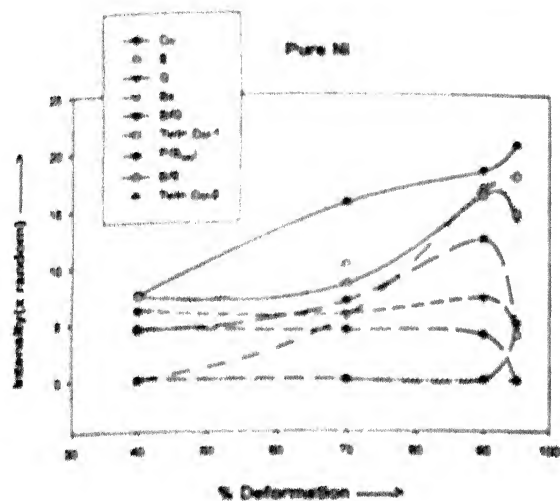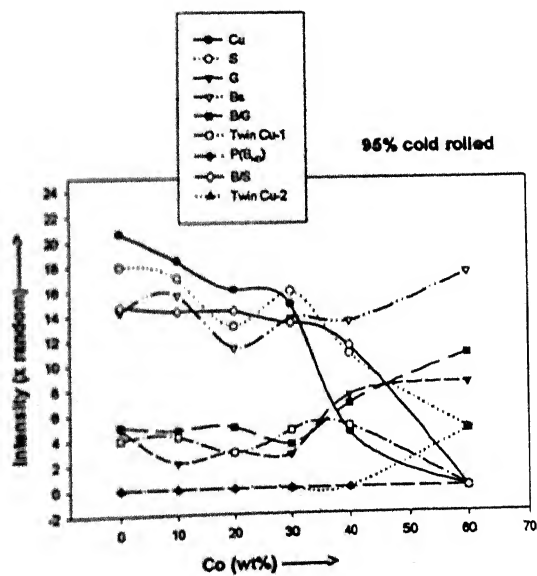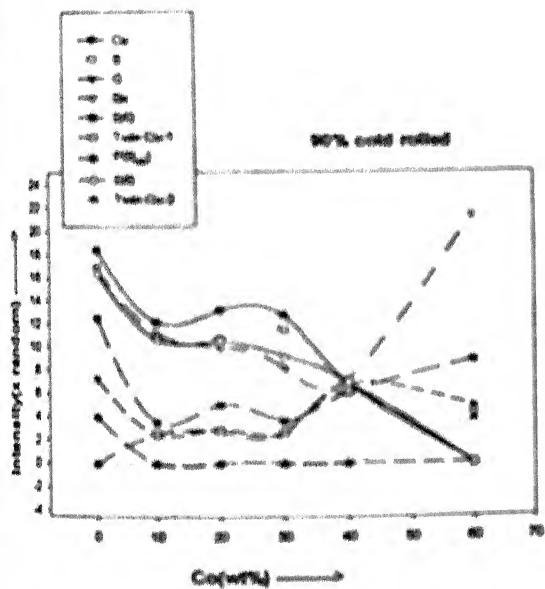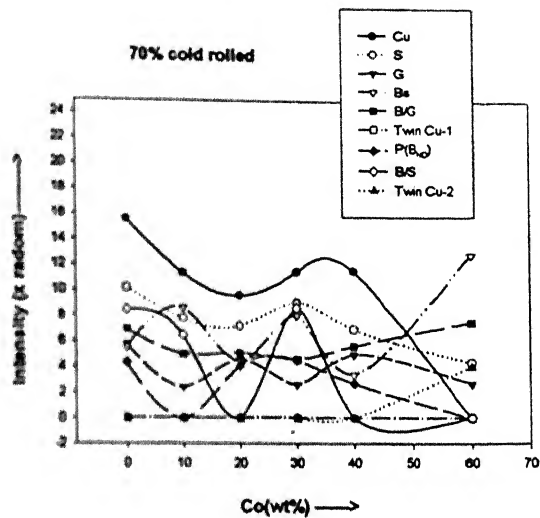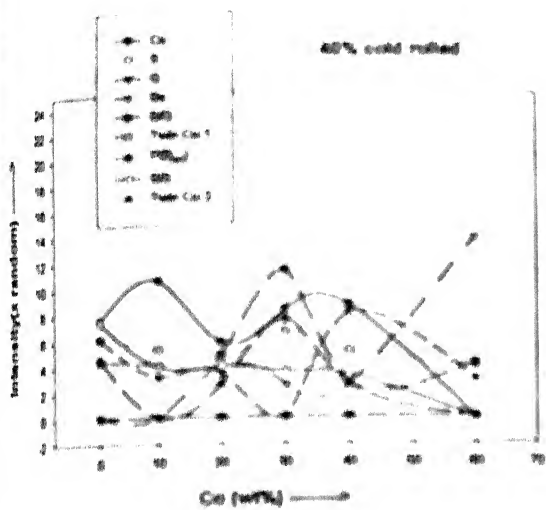
Figure 4.30   Plots showing the variation in peak intensity, with wt% Co, of the various texture components at particular deformations.

Chapter 5

Discussion

The {111} pole figures and also the composite texture ODF section plots show the similarity of texture developed on cold rolling at any deformation level in pure Ni and Ni-Co alloys upto 30%Co. The textures in these alloys are similar to those developed in cold rolled Cu. The textures developed in Ni-60%Co are completely different and match with those reported for cold rolled α- brass. The {111} pole figures and ODF plots of Ni-40%Co reveal an intermediate texture which is a mixture of Cu type and α- brass type.

The α,β and τ fibres also reveal the transition in texture developed in the series of Ni-Co alloys under study. Upto Ni-30%Co the Bs, Cu and S peaks are strong in all cases, each component increasing in intensity with increasing in the amount of deformation. The Cu type textures in alloys upto Ni-30%Co undergo change with further addition of Co and, infact, show a transition to α- brass type texture in Ni-40%Co. In this alloy the Cu peak reduces in intensity while the Bs peak sharpens with increasing levels of deformation. The S component is still strong in intensity in the Ni-40%Co. The rolling textures developed in Ni-60%Co are completely different from the above with Cu absent and S considerably weak and a highly developed Bs peak. The α- brass type texture appears to form in Ni-60%Co at an early stage of deformation and then develops further with increasing deformation. The β skeleton line shows different positions in the different Ni-Co alloys ; however the positional shift of this lines, as a function of Co content, is

lesser when the deformation level is higher. Thus at 95% deformation, the β skeleton line in all alloys irrespective of Co content occupies similar position.

The deformation textures developed in fcc metals and alloys have been found to be very strong functions of the stacking fault energies of the materials. Pure Ni with 130mJ/m² SFE falls in the group of medium SFE metals and aquires Cu type texture on cold rolling. Materials in the low stacking fault energy group have α–brass type texture. Additions of Co to Ni brings about a decrease in SFE. Table 5.1 shows the approximate SFE values for pure Ni and Ni-Co alloys as reported by Gallagher[4].

Table 5.1   Stacking fault energy of pure Ni and Ni-Co alloys.

Material	Stacking Fault Energy(mJ/m^2)
Pure Ni	130
Ni-10Co	113
Ni-20Co	91
Ni-30Co	71
Ni-40Co	52
Ni-60Co	13

It is evident that the drastic reduction in SFE of Ni brought about by Co is sufficient to initiate texture transition from Cu type to α brass type in cold rolled Ni-Co alloys. Similar work done on a series of Ni-Fe alloys [2,52] has revealed no transition in texture from Cu type to α brass type on Fe addition. In the latter case the minor reduction in SFE of Ni brought about by Fe additions upto 40 wt% (from 130 to 101mJ/m²) was not sufficient enough to initiate texture transition.

The transition in rolling texture observed in Ni-Co alloys matches quite well with similar texture transition in the Cu-Zn system, investigated by Hirsch and Lücke[3]. The

nature of change in the α,β and τ fibres in this series is same as that for Cu-Zn system . Figs 5 1, 5 4 show the α, β & τ fibre plots for pure Ni, Cu[3], Ni-Fe[52] & Ni-Co alloys. The α fibre plots (Fig 5 1) for Ni-Co alloys show similar nature as in Cu-Zn alloys with intensity maxima at the Bs position The transition in texture from Cu type to α brass type is evident in the τ fibre plots (Fig 5 2) Ni-60%Co shows a highly reduced peak at the Cu position as compared to the other Ni-Co alloys as well as in the Ni-Fe alloys[52]. The decrease in the Cu peak intensity is accompanied by an increase in the G orientation. Similar differences are observed in the τ fibre plots of Cu-30% Zn alloy vis-a-vis pure Cu The β fibre plots(Fig 5 3) of Ni-60%Co and Cu-30%Zn are also similar showing a highly reduced Cu intensity and a very strong Bs peak. The nature of the β fibre is quite different in the above alloys as compared to that in pure Ni, Cu and Ni-Fe alloys. Thus it is clear from the comparison of the texture fibre plots that the texture transition in Ni-Co system is very similar to that in the Cu-Zn system. Whereas in the Cu-Zn system 5%Zn initiates texture transition, in the Ni-Co system such initiation is observed for 40%Co. No transition in rolling texture as is observed for the Ni-Co system has been reported for the Ni-Fe system[2,52] This is believed to be due to the wide difference in the behaviour of Co and Fe in reducing the SFE in pure Ni. SFE in pure Ni by Co & Fe respectively.

Wassermann[41] had proposed a mechanism of rolling texture transition from pure metal type to α brass type through mechanical twinning. His "twin hypothesis" proposes that the Cu orientation {112}<111> transforms by twinning to the Twin Cu orientation {552}<115> which rotates to the G orientation {110}<001> by subsequent slip. The course of texture transition in Ni-Co alloys seems to support Wassermann's

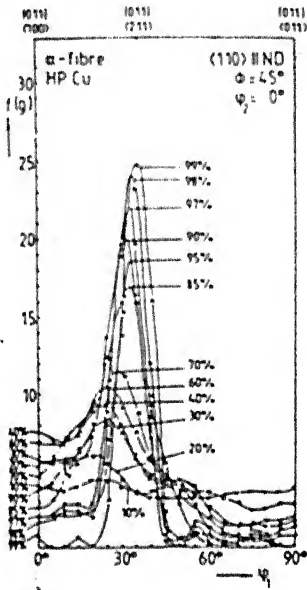nature of change in the α, β and τ fibres in this series is same as that for Cu-Zn system .

Figs 5.1-5.4 show the α, β & τ fibre plots for pure Ni, Cu[3], Ni-Fe[52] & Ni-Co alloys.

The α fibre plots (Fig 5.1) for Ni-Co alloys show similar nature as in Cu-Zn alloys with

intensity maxima at the Bs position. The transition in texture from Cu type to α brass

type is evident in the τ fibre plots (Fig 5.2). Ni-60%Co shows a highly reduced peak at

the Cu position as compared to the other Ni-Co alloys as well as in the Ni-Fe alloys[52].

The decrease in the Cu peak intensity is accompanied by an increase in the G orientation.

Similar differences are observed in the τ fibre plots of Cu-30% Zn alloy vis-a-vis pure

Cu. The β fibre plots(Fig 5.3) of Ni-60%Co and Cu-30%Zn are also similar showing a

highly reduced Cu intensity and a very strong Bs peak. The nature of the β fibre is quite

different in the above alloys as compared to that in pure Ni, Cu and Ni-Fe alloys. Thus it

is clear from the comparison of the texture fibre plots that the texture transition in Ni-Co

system is very similar to that in the Cu-Zn system. Whereas in the Cu-Zn system 5%Zn

initiates texture transition, in the Ni-Co system such initiation is observed for 40%Co.

No transition in rolling texture as is observed for the Ni-Co system has been reported for

the Ni-Fe system[2,52]. This is believed to be due to the wide difference in the behaviour

of Co and Fe in reducing the SFE in pure Ni. SFE in pure Ni by Co & Fe respectively.

Wassermann[41] had proposed a mechanism of rolling texture transition from

pure metal type to α brass type through mechanical twinning. His "twin hypothesis"

proposes that the Cu orientation {112}<111> transforms by twinning to the Twin Cu

orientation {552}<115> which rotates to the G orientation {110}<001> by subsequent

slip. The course of texture transition in Ni-Co alloys seems to support Wassermann's
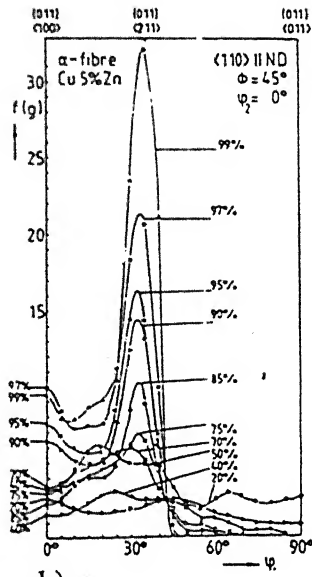
hypothesis. With reduction in the intensity of the Cu orientation in Ni-60%Co, a new maxima is observed at the {552}<115> position in the τ fibre plot along with an increase in intensity of the G position (Fig 4.20). Such nature of τ fibre is also observed for Cu-30%Zn (Fig 5.2).

Although the textures developed in Ni-60%Co and in Cu-30%Zn are both α brass type, there are differences in the relative weightages of the relevant components. Whereas in case of Ni-60Co the S component occupies high volume fraction at all deformations, it is relatively low and reduces with increasing deformation in Cu-30%Zn (Fig 5.5). The volume fraction of the main component Bs in Ni-60%Co reduces with increasing deformation, but in case of Cu-30%Zn a continuous increase in volume fraction of this component with deformation is observed.
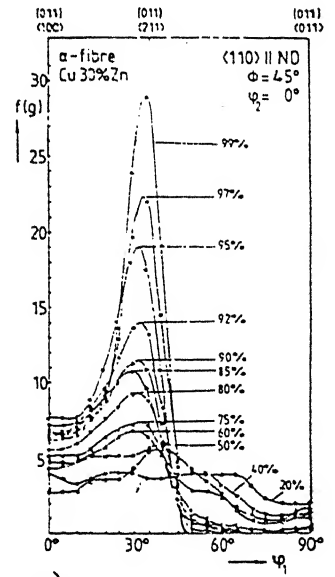
The micrographs from the longitudinal sections reveal the deformed structures which are not very different from alloy to alloy. The grains are distinguishable upto 70% deformation and have twins as well as deformation bands within them. The grains at 70% deformation are more elongated ,as is expected than at 40% deformation. No grains are visible at 90 and 95% deformation where the structure is highly fragmented with profusion of deformation bands.

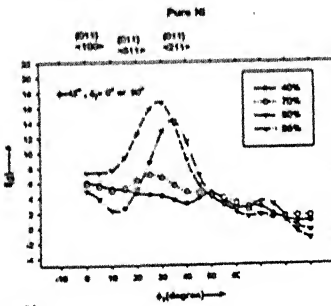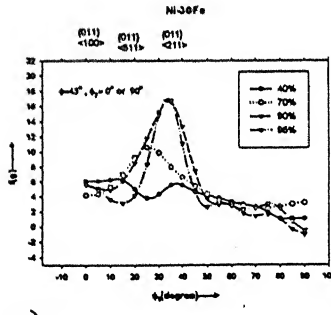Figure 5.1   Comparison of α fibre plots: a) pure Cu, b) Cu-5%Zn, c) Cu-30%Zn, d) pure

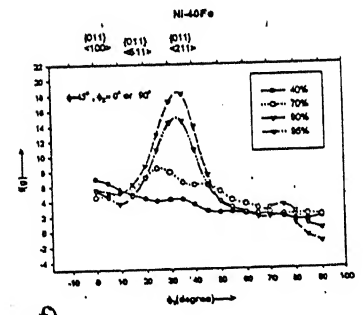Figure 5.2   Comparison of τ fibre plots: a) pure Cu, b) Cu-5%Zn, c) Cu-30%Zn, d) pure

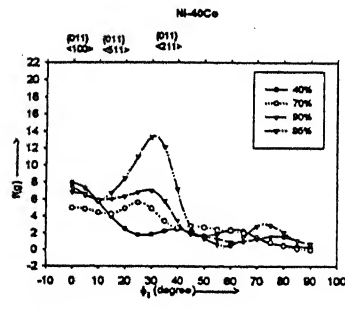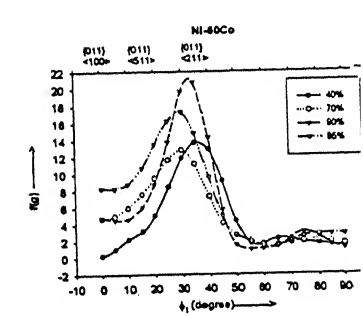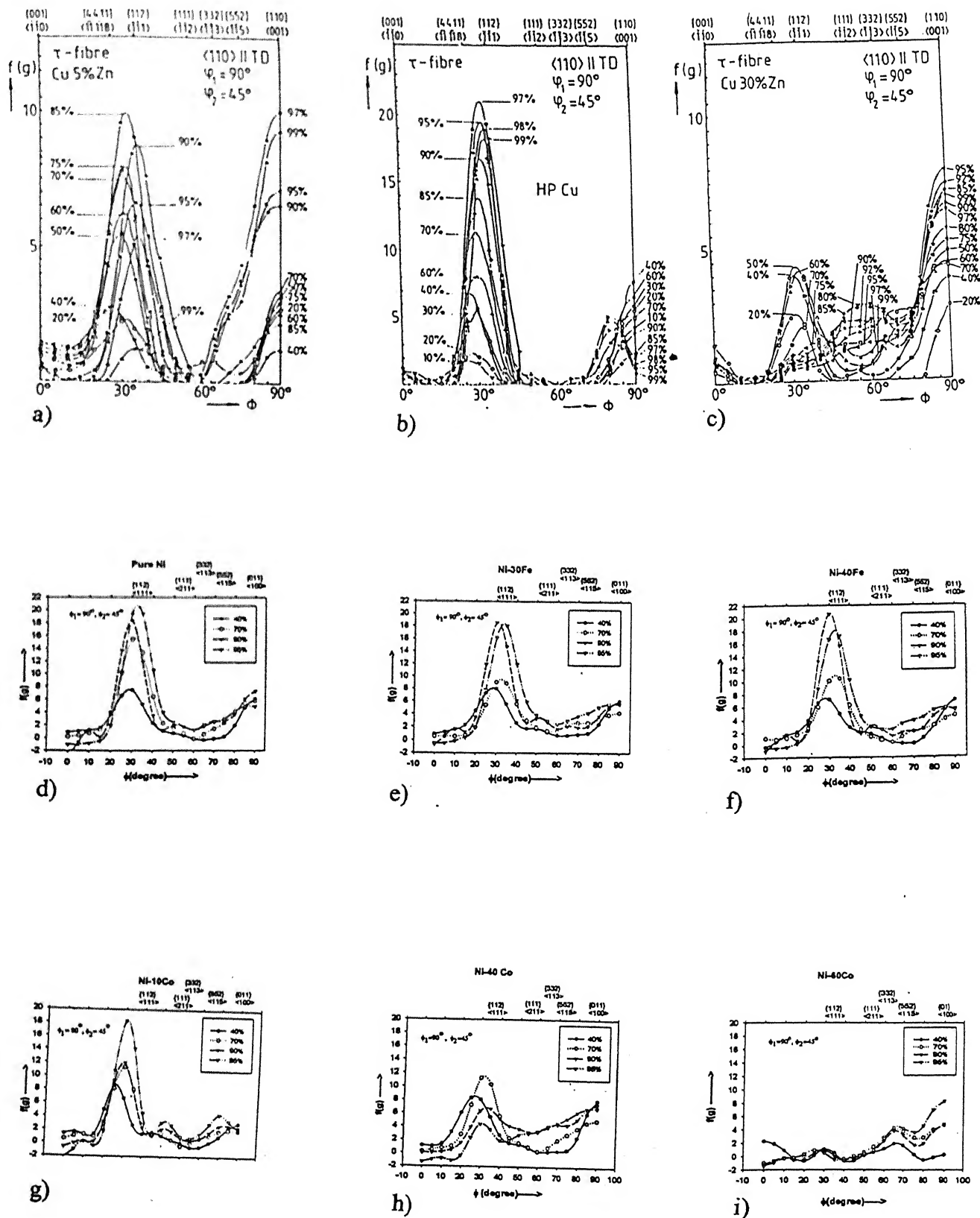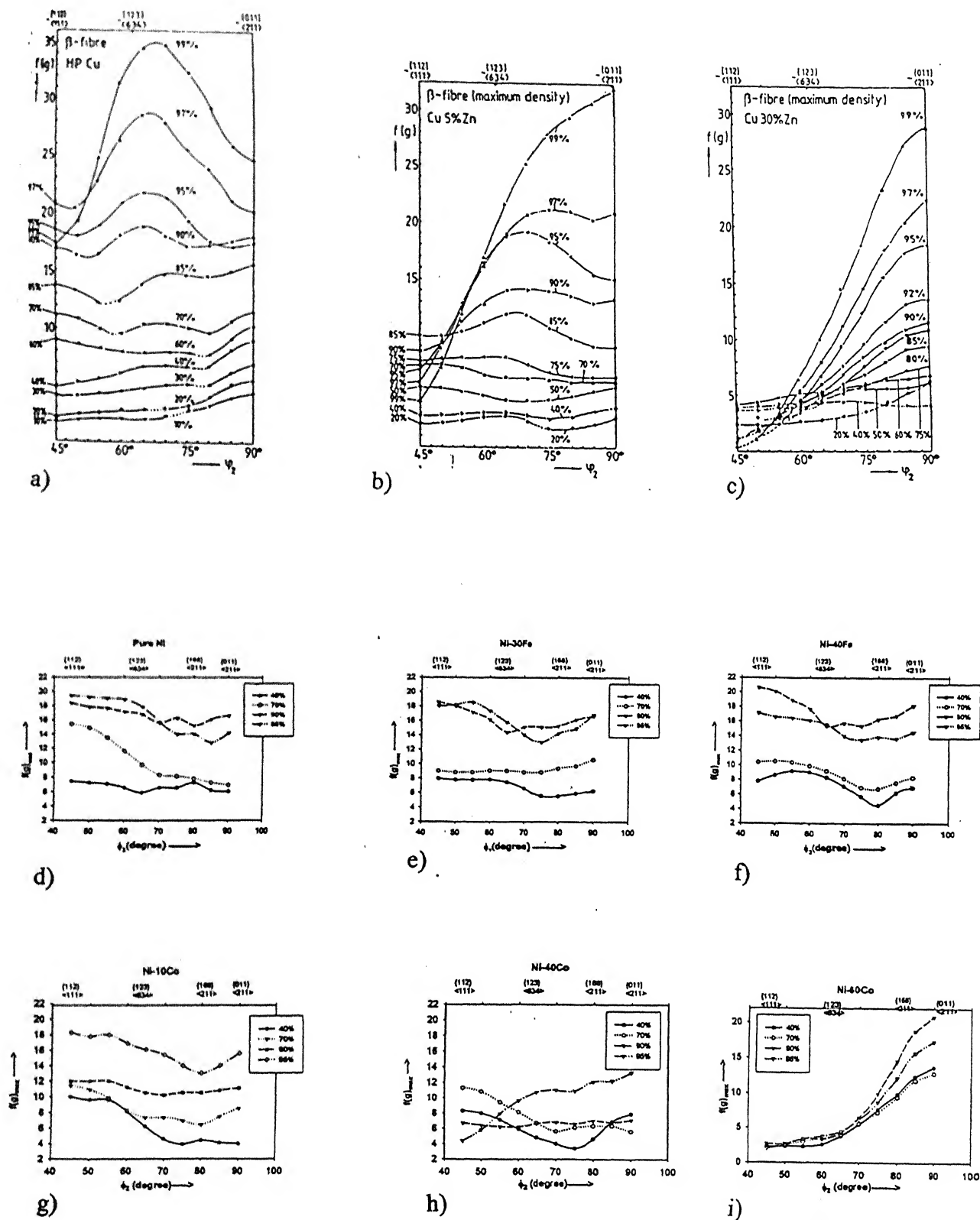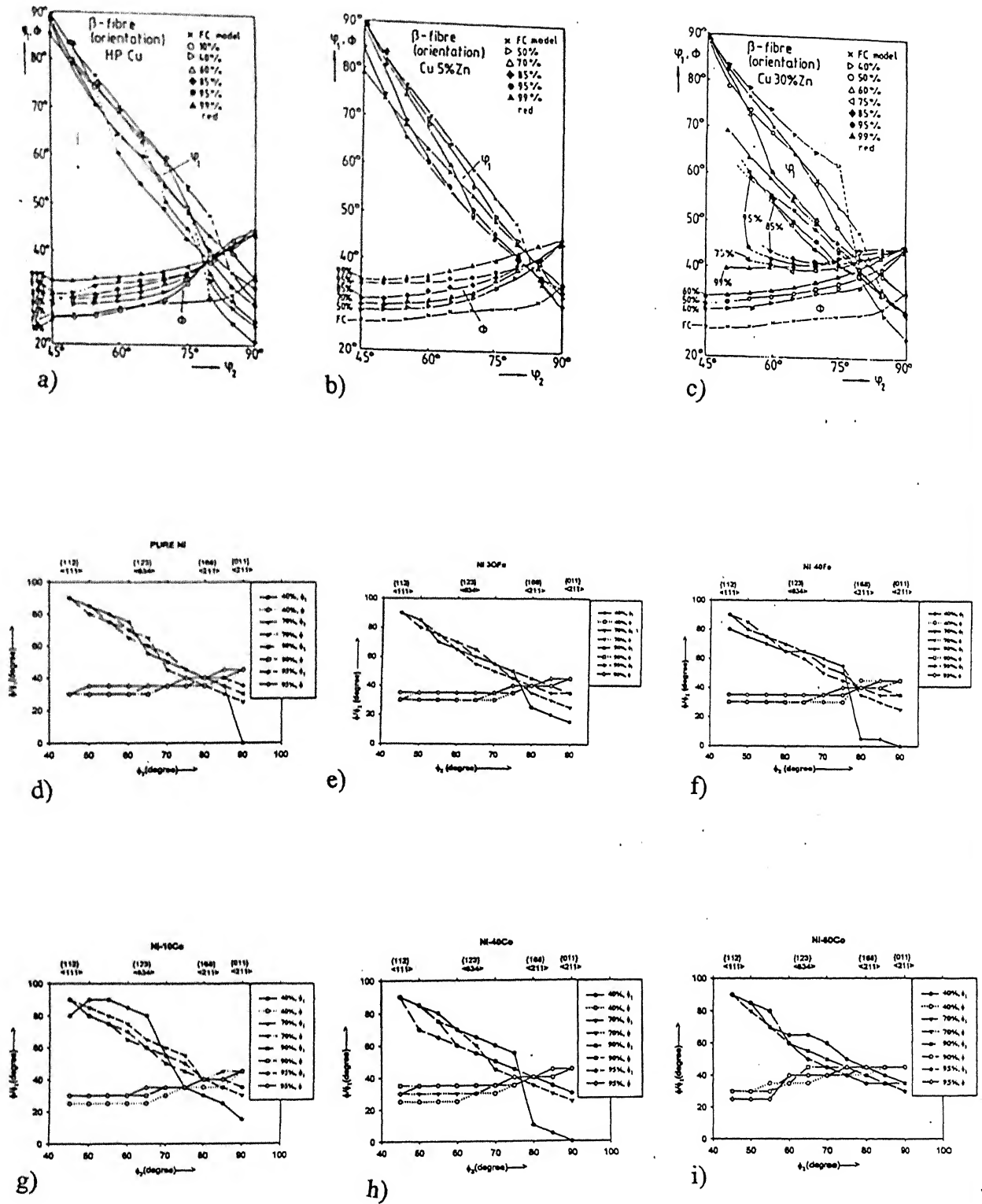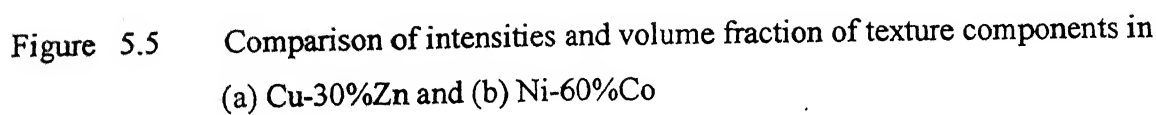Figure 5.3   Comparison of β fibre plots: a) pure Cu, b) Cu-5%Zn, c) Cu-30%Zn ,d) pure
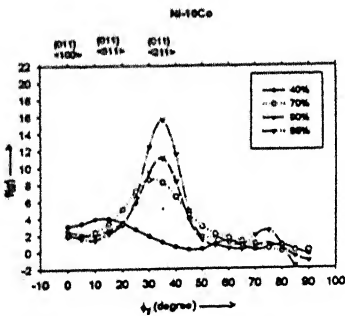
Figure 5.4 Comparison of course of β fibres in:a) pure Cu, b) Cu-5%Zn, c) Cu-30%Zn ,d) pureNi, e) Ni-30%Fe, f) Ni-40%Fe, g) Ni-10%Co, h) Ni-40%Co,i) Ni-60%Co

(a)

(b)

Figure 5.5   Comparison of intensities and volume fraction of texture components in
(a) Cu-30%Zn and (b) Ni-60%Co

Chapter 6

Conclusions

- The texture developed on cold rolling in Ni-Co alloys with upto 30%Co is pure metal or Cu type, similar to that developed in pure Ni.

- Ni-60%Co shows α brass or alloy type texture.

- Ni-40%Co develops an intermediate texture having a mixture of pure metal type as well as α brass type character.

- Increasing deformation strengthens the pure metal type texture developed in alloys with upto 30%Co and the α brass type texture developed in Ni-60%Co.

- The texture in Ni-40%Co is found to shift from pure metal type to α brass type with increasing deformation.

- The texture transition in Ni-Co system is found to be similar to that developed in the Cu-Zn system.

- Although the rolling texture of Ni-60%Co and Cu-30%Zn are both α brass type, there are differences in the relative weightages of the relevant components.

- The main texture components for the Cu type texture are Cu, S & Bs. The other components identified are G, B/G, B/S, P(B_{ND}) & Twin Cu.

- The main component for α brass type texture in Ni-60%Co is Bs. The other components identified are B/G, G, S & Twin Cu.

- The microstructures in pure Ni and all Ni-Co alloys are similar at any particular deformation level.

References

1. Peter Haasen, *Physical Metallurgy*, Cambridge University Press, Cambridge (1978).

2. R.K.Ray, *Acta Metall. Mater.* **43**, 3861 (1995).

3. J. Hirsch and K. Lücke, *Acta metall.* **36**, 2863 (1988).

4. P. C. J. Gallagher, *Metall. Trans.* **1**, 2429 (1970).

5. Samuel J. Rosenberg, *Nickel and its Alloys*, National Bureau of Standards Monograph 106, May (1968).

6. J. G. Byrne, *Recovery, Recrystallisation and Grain Growth*, 1 (1965), The Macmillan co., New York.

7. Hatherly M. and Huchinson W.B., *An Introduction to Textures in Metals*, The Institution of Metallurgists, Monograph No. 5, (1979).

8. H. J. Bunge and F. Haessner, *J. Appl. Phys.*, **39**, 5503 (1968).

9. R. J. Roe, *J. Appl. Phys.* , **36**, 2024 (1965).

10. H. Hu, P. A. Beck, *J. Metals*, **2**, 1214 (9150).

11. H. Hu, P. R. Sperry and P. A. Beck, *Trans. A.I.M.E.*, **194**. 76 (1952).

12. R. E. Smallman, *J. Inst. Met.* , **84**, 10 (1955-56).

13. F. Haessner, *Z. Metallkunde*, **53**, 403 (1962).

14. F. Haessner, *Z. Metallkunde*, **54**, 79 (1963).

15. M. Hatherly, *J. Austr. Inst. Met.* , **8**, 140 (1963).

16. K. Detert, P. Dorsch and H. Migge, *Z. Metallkunde*, **54**, 263 (1963).

17. R. H. Richman and Y. C. Lin, *Trans. A.I.M.E.* , **221**, 720 (1961).

18. R. H. Richman and Y. C. Lin, *Trans. A.I.M.E.* , **218**, 668 (1960).

19. R. E. Smallman, *J. Inst. Met.* , **83**, 408 (1954-55).

20. C. S. Barrett, *The Structure of Metals*, 2nd edn. , 1952, New York (McGraw-Hill).

21. E. R. W. Jones and E. A. Fell, *Acta Met.*, **5**, 689, (1957).

22. K. Lucke, H. Perlwitz and W. Pitsch, *Phys. Stat. Sol.*, **7**, 733, (1964).

23. F. Heassner, U. Jakubowski and M. Wilkens, *Phys. Stat. Sol.* , **7**, 701, (1964).

24. C. A. Clark and P. B. Mee, *Z. Metallkunde*, **53**, 756 (1962).

25. I. L. Dillamore, R. E. Smallman and W. T. Roberts, *Phil. Mag.*, **9**, 517, (1964).

26. I. L. Dillamore and W. T. Roberts, *Met. Rev.*, **10**, 271 (1965).

27. H. Hu, R. S. Cline and S. R. Goodman, *J. Appl. Phys.*, **32**, 1392 (1961).

28. H. Hu and S. R. Goodman, *Trans. A.I.M.E.*, **227**, 627 (1963).

29. H. Hu and S. R. Goodman, *Trans. A.I.M.E.*, **230**, 1413 (1964).

30. R. E. Smallman and D. Green, *Acta Met.*, **12**, 145 (1964).

31. F. A. Underwood, *Textures in Metal Sheet*, London (Macdonald), (1961).

32. H. Hu, R. S. Cline and S. R. Goodman, *Recrystallisation Grain Growth and Textures*, 295 (1966), A.S.M., Metals Park, Ohio.

33. F. Haessner, *Recrystallisation Grain Growth and Textures*, 386 (1966), A.S.M., Metals Park, Ohio.

34. F. Haessner, *Z. Metallkunde*, **54**, 98 (1963).

35. T. Richards and S. F. Pugh, *J. Inst. Met.*, **88**, 399 (1959-60).

36. Y. C. Liu, *Trans. A.I.M.E.*, **230**, 656 (1964).

37. I. L. Dillamore and W. T. Roberts, *Acta Met.*, **12**, 281 (1964).

38. G. Schöck and A. Seeger, *Defects in Crystalline solids*, The Physical Society, london, 340 (1955).

39. H. Wolf, *Z. Naturforsch*, **15a**, 180 (1960).

40. F. B. Hirsch, *Phil. Mag.*, **7**, 67 (1963).

41. G. Wassermann, *Z. Metallkunde*, **54**, 61 (1963).

42. P.R.Thronton and T.E. Mitchell, *Phil. Mag.*, **7**, 371 (1962).

43. H. J. Bunge, *Mathematische Methoden der Textur- analyse*. Academic Press, Berlin (1969).

44. J. Jura and J. Pospiech, *Textures 3*, 1 (1978).

45. W. Truszkowski, J. Pospiech, J. Jura and B. Major, *Proc Zeme Coll. Europeen Sur Text.* Pont-a-Mousson, France (1973).

46. K. Lücke, J. Pospiech, K. H. Virnich and A. Flemmer, *Proc. Fifth Int. Conf. Text.* **1**, 129 (1978).

47. J. Hirsch and K. Lücke, *Acta metall.* **33**, 1927 (1985)

48. J. Hirsch and K. Lücke, *Theoretical Methods of Texture Analysis* (edited by H. J. Bunge) p. 53. D.G.M. Oberursel (1987).

49. K. Lücke, J. Pospiech, K. H. Virnich and J. Jura, *Acta metall.* **229**, 167 (1981)

50. H.J. Bunge and J. Tobisch, *Z. Metallkunde*, **59**, 471 (1968).

51. K.H. Virnich, *Phd dissertation*, Institut für Metallkunde, R.W.T.H. Aachen, Germany (1979)

52. R. Prasad, *M. Tech Thesis*, IIT Kanpur (1999).

A 130841

A 130841